DESIGN DEVELOPMENT AND ANALYSIS OF A DUAL MODE FREE PISTON JET ENGINE WITH APPLICATIONS TO LIGHT AIRCRAFT

by

DAVID L. AKIN

B.S., Massachusetts Institute of Technology

(1974)

SUBMITTED IN PARTIAL FULFILLMENT

OF THE REQUIREMENTS FOR THE

DEGREE OF MASTER OF SCIENCE

at the

MASSACHUSETTS INSTITUTE OF TECHNOLOGY

June, 1975

Signature of author ____________________

Department of Aeronautics and Astronautics

May 9, 1975

Certified by ____________________

Thesis Supervisor

Accepted by ____________________

Chairman, Departmental Graduate Committee

DESIGN DEVELOPMENT AND ANALYSIS OF A DUAL MODE FREE PISTON JET ENGINE WITH APPLICATIONS TO LIGHT AIRCRAFT

by

DAVID L. AKIN

Submitted to the Department of Aeronautics and Astronautics on May 9, 1975, in partial fulfillment of the requirements for the degree of Master of Science.

ABSTRACT

The design of the free piston jet engine is traced through the stages of development. The dual mode modification is introduced, examined, and applied. The final design iteration is analyzed from the basis of work equilibrium, and cycle performance is combined with engine geometric and thermodynamic detail to give performance calculations. All calculations are nondimensionallized, and a trend analysis performed on the inlet conditions. A prototype flight engine, using Volkswagen cylinders, is designed and analyzed.

Thesis Supervisor: Jack L Kerrebrock
Title: Professor of Aeronautics
and Astronautics

ACKNOWLEDGEMENTS

I would like to thank Professor Jack L. Kerrebrock for his aid, advice, guidance, and suggestions which he has given me on the project for the last two years. I particularly want to thank him for those immortal words, "You know, Dave, when you first came in here last year with the idea for this project, I really thought it was a crazy thing to do. I still do, but it is interesting." To which I can only add, "Amen."

TABLE OF CONTENTS

Figures		Page No.

Tables

NOMENCLATURE

Variables

a	dimensionless area, A/X_e^2
c_p	specific heat at constant pressure
d	dimensionless diameter
e	density ratio, ρ_{pt}/ρ_a
f	dimensionless thrust
k	adiabatic constant (= 1.4)
l	dimensionless length, L/X_e
m	dimensionless mass
p	engine supercharge pressure ratio, P_1/P_a
q	dimensionless half-cycle period
sfc	dimensionless specific fuel consumption
t	combustion temperature ratio, T_b/T_s
u_e	dimensionless exhaust velocity
v	dimensionless volume
w	dimensionless work, $W/P_aX_e^3$
x	dimensionless distance, X/X_e
A	area
C*	characteristic velocity
D	diameter
F	thrust
L	piston travel length
M	mass

P pressure

Q half-cycle period

R gas constant

SFC specific fuel consumption

T temperature

U_e exhaust velocity

V volume

W work

X distance

ρ density

Subscripts

a ambient

b combustion

c combustion chamber

com compression

e combustion chamber exhaust

ep pump chamber exhaust

exp expansion

m combustion chamber minimum

mp pump chamber minimum

mx combustion chamber maximum

mxp pump chamber maximum

o internal condition, pump chamber exhaust p pump chamber

pt piston

t nozzle throat

1 combustion chamber intake condition

3 post-combustion combustion chamber condition

Superscripts

$\cdot$ time derivative

$-$ average value

CHAPTER 1

INTRODUCTION

1.1 Origin

The origin of the dual mode free piston jet engine lays in the combination of a need and an idea. The need stretches back before World War II, the idea from the end of the last decade.

Since before the first successful powered flight of an aircraft, people have been predicting an age of the universal use of air vehicles for personal transportation. Depending upon the source, the vision may have varied between widespread extension of the neighborhood airport system and a vertical takeoff and landing supersonic personal family runabout in every garage; yet all such plans predicted a widespread movement to personal air transportation, such as happened in an earlier age with the advent of the personal automobile. Yet, no such movement has materialized. Out of a nation of over two hundred million people, the Federal Aviation Administration reports only 650,000 currently licensed pilots, with slightly over one hundred thousand planes in the civil air fleet. Aircraft are still made on an individual basis, using little of the mass production knowledge gained by automobile manufacturers over the last decades. Airframe manufacturers aim their advertising at the business community; the phrase "write on your company stationary" is appearing on more and more advertisements in aviation magazines. Few speak any longer of the age of personal air transportation.

While the complete list of causes of this trend vary with personal opinion, there is no question that monetary factors rate close to the top of all the lists. According to the Aerospace Specification Tables of the March 17, 1975 issue of Aviation Week and Space Technology, the lowest standard list price of any American production aircraft is $10,700, for the Cessna 150. The Cessna 172 Skyhawk sold 1786 units in 1974, making it the largest selling aircraft model of the year. The current list price for the 172, with only basic flight instruments, is $17,890. It is not uncommon for the cost of avionics to increase the cost of such a plane by between fifty and one hundred percent.

Shortly after World War II, the advent of jet propulsion for military aircraft spurred visions of a new wave of jet-powered personal aircraft. However, the myriad parts of the modern turbofan engine place it outside the price range of all but the more wealthy corporations. The least expensive turbofan aircraft available at this time, again according to Aviation

Week, is the Cessna 500 Citation, which lists for $795,000.

One attempt to alter this condition is the BD-5J, a small single-seat jet plane currently being certified by Bede Aircraft. This $26,000 aircraft is powered by a French Sermel TRS-18 jet engine. According to Jane's All The World's Aircraft, 1973-74, the TRS-18 is a turbojet engine, with a single stage centrifugal compressor and an axial turbine, also single stage. The engine weighs 66 pounds with an electric starter, produces 200 pounds thrust at sea level, and drinks 1.45 pounds of fuel per hour, per pound of thrust. At rated maximum cruise thrust of 190 pounds, this corresponds to a fuel flow rate of 275 pounds per hour. Thus, the price of a jet engine in the BD-5J is both the initial cost, on the order of $20,000, and the operational costs of 275 pounds of JP-4 fuel for every hour of flight.

What, then, would be the characteristics of the optimum light aircraft powerplant? It should be extremely simple, to lower both the initial costs and the maintenance costs. It should be lightweight, easy to integrate into the airframe, and have a low specific fuel consumption, to keep fuel costs at a reasonable level. It should be made from common, inexpensive materials, and the configuration should lend itself to construction with the least possible number of manufacturing steps. It should have the performance capabilities of a jet engine with the fuel efficiency of a reciprocating engine driving a propeller.

1.2 Design Development

The idea of a free piston jet engine originated in one of the popular magazines on mechanics, sometime in the late 1960's. Several literature searches have failed to disclose the issue, or even the title of the magazine, so the original configuration of the engine is taken only from memory.

The engine described in the article consisted of two solid cylindrical pistons, rigidly connected by a rod passing through a seal in a barrier separating the two cylinders. An acetylene-air mixture was burned in the combustion chambers, and expanded through a nozzle to provide thrust. A spark ignition system was provided for starting, but was disabled after the engine was running, allowing the engine to continue with compression ignition. Water was injected into the exhaust stream in the nozzle, and a sizable fraction of the thrust was probably provided by this water injection. Typically for articles of this type, the performance is measured in barely quantitative terms; in this case, the engine was mounted on the back of a go-cart, which was then clocked at speeds up to 120 miles per hour. This indicates a thrust level which would begin to be of interest for light aircraft propulsion systems; yet the engine is not really usable in such a system, for a number of reasons. Fuel availability, specific fuel consumption increases due to water injection, fuel feed, all of these suggested the need for a more efficient system, with the thrust advantages of the free piston jet engine.

The original design left room for various improvements. For light aircraft, the use of acetylene as a fuel was clearly unacceptable. Not only would heavy pressure cylinders have to be carried, but also an aircraft engine is useless if the fuel for it cannot be procured at the airport. Water injection was similarly ruled out, since the high specific fuel consumption would have severely limited the range of the aircraft for a given gross takeoff weight.

The first design studied consisted basically of normally configured pistons with a straight connecting rod. As is usually done in two-stroke engines, a fuel-air-oil mixture would be drawn into the volume behind the piston as the combustion chamber compression stroke advanced, and would be compressed on the expansion stroke. The exhaust products would be expanded through a nozzle in order to provide thrust, and the fuel-air mixture is then ported into the combustion chamber, to scavenge the exhaust products and act as reactants for the next combustion cycle. A computer program was written to simulate the motion of the piston, by successively resolving the pressures in each of the chambers, solving for total force acting on the piston, and numerically integrating for piston velocity and position. It was found from this computer simulation that the cycle was divergent for all combinations of geometric and thermodynamic variables.

At this point, another analysis was made from the viewpoint of work equilibrium, which disclosed that each chamber produced a positive net work in a cycle. Since no mechanical work is extracted from the piston, and friction is assumed to be negligible, the only way this work could be extracted in a stable cycle is if it is used for compression of the other cylinder. However, since the engine is symmetric, a stable solution exists for the cycle only if the net work of the modelled Otto cycle is zero, corresponding to no combustion and zero piston movement. All other solutions possessed a net half-cycle work, driving the piston cycle divergent.

It seems obvious that the two straightforward solutions to prevent the divergent cycle would be to either provide for extraction of the excess mechanical work or to eliminate the symmetry of the engine.

The next design, after a suggestion by Professor J. L. Kerrebrock, used both of the above solutions. The engine was made unsymmetrical, with a combustion chamber at one end, and a larger compression chamber at the other. The purpose of this "pump" chamber is to draw in air at atmospheric pressure, compress it, and expand it without combustion through a nozzle to provide thrust. This engine directly corresponds to a turbofan engine, in which a large mass of air is drawn in, compressed, and expanded to provide thrust, while a relatively smaller amount of air is mixed with fuel and burned in order to provide power to the engine. The pump chamber exhaust nozzle on the free piston jet engine would only be open above a certain pressure, and residual pressure in the pump chamber after the exhaust valve closes would provide the power necessary to compress the combustion chamber for the next cycle. The presence of the two separate and distinct chambers, the pump and combustion chambers, is the essential dual mode modification, which should greatly improve the propulsion system efficiency, in particular the specific fuel consumption.

However, this engine also had design faults. While the combustion chamber expansion stroke was rapid, the low residual pressure in the pump chamber caused a much slower compression stroke in the combustion chamber. It not only had to work against the adiabatically increasing combustion chamber pressures, but also against the constant atmospheric pressure against the back face of the pump piston. Combined with the adiabatically decreasing pressure in the pump chamber forcing compression, the compression ratios attainable were too low (on the order of 1.2:1) to be of any practical use. Also, the use of pressure actuated valves in the exhaust nozzles provided both an increase in complexity and a pressure drop across the valve, increasing costs and decreasing performance.

For these reasons, the design was returned to a symmetrical one, of cruciform axial section. A combustion chamber on each end provides net work, to be absorbed by two annular pump chambers, which provide a high volume air flow for thrust. A duct porting arrangement is designed into the piston to provide pump chamber exhaust at high compression ratios without the large pressure drops of valves in the nozzle flow. An additional feature of this configuration is that high pressure air may be tapped from the pump chambers, to provide a convenient source of pressure for combustion chamber supercharging.

While providing an improvement on the previous engine designs, this design is not readily applicable to the analysis scheme. It is therefore modelled as having a cylindrical piston, with an "actuator disc" pump piston face of zero width. This is possible, since the actual portion of the piston which provides pump compression and porting displace a constant volume of the pump chambers. In conjunction with this, an effective exhaust volume V_{ep} is defined, which represents the volume contained between the pump piston face and cylinder head at the point at which the exhaust port is uncovered.

The final design change represents merely a refinement of detail over the last revision. The piston configuration is changed from a cruciform axial section to a hollow cylindrical pump piston containing the ducting ports, and connected by rods to skirted pistons in each of the combustion chambers. Also, the ducting in the pump piston is made concentric instead of successive in the axial direction, which greatly shortens the pump piston. All of these changes combine to provide a large reduction in piston size and weight.

CHAPTER 2

ANALYSIS

2.1 Cycles

In order to perform engine analysis on the basis of total work, it is necessary to find thermodynamic cycles which approximate the actual pressure-volume time history in the cylinders. The combustion chamber at each end of the engine is similar in configuration to most internal combustion engines, and an air-standard Otto cycle is therefore assumed, with modifications due to porting arrangement. Referring to figure 6, the cycle starts at point 0, corresponding to piston rest at bottom dead center. As the piston moves on the compression stroke, the pressure remains constant until the exhaust port is covered at point 1, at which point chamber volume is V_e. The fuel-air mixture is then compressed adiabatically until piston rest occurs at V_m, top dead center. It should be emphasized that the major difference between the cycle of a normal internal combustion engine and that of the combustion chamber for the dual mode free piston jet engine is that the compression ratio of the jet engine, V_e/V_m, is not constrained by engine geometry. A standard internal combustion engine operates at only one compression ratio, set by the configuration of connecting rods and crankshaft. Compression ratio of a free piston engine depends on thermodynamic and engine sizing parameters.

At top dead center, combustion is modelled as a constant volume heat addition, resulting in a chamber pressure rise to point 3. The piston then moves on the expansion stroke, with the chamber pressure dropping adiabatically until the inlet and exhaust ports are uncovered at point 4. The chamber pressure then drops to inlet pressure P_1, and chamber scavenging and recharging takes place throughout the rest of the stroke.

The pump chamber pressure-volume relationship is also modelled as an air-standard cycle. From rest at bottom dead center, pressure increases adiabatically on the compression stroke until the exhaust nozzle is uncovered, at which point the pressure drops back to atmospheric. It continues at atmospheric throughout the rest of the stroke and all of the return stroke, as atmospheric air is drawn into the pump chamber for replenishment. This cycle can be seen in figure 7. It should be noted that for each of these cycles, both of the corresponding chambers are undergoing identical cycles at each end of the engine, one hundred and eighty degrees out of phase.

2.2 Work Equilibrium and Performance Analysis

For air-standard cycles, the mechanical work available is equal to $\int PdV$. Looking at the combustion chamber cycle, the compression work is equal to

$$W_{com,c}=W_{0-1}+W_{1-2} \tag{1}$$

From point 0 to point 1, the pressure is constant at the supercharge pressure P_1. Once the exhaust port is covered at point one, the pressure increases adiabatically until the end of the stroke at point 2. The work done by the piston is

$$W_{com,c}=\int_{V_{mx}}^{V_e} PdV + \int_{V_e}^{V_m} PdV \tag{2}$$

Using the fact of constant pressure and the adiabatic relation for a perfect gas,

$$W_{com,c}=\int_{V_{mx}}^{V_e} P_1 dV + \int_{V_e}^{V_m} P_1 \left(\frac{V_e}{V}\right)^k dV \tag{3}$$

Integrating gives

$$W_{com,c}= P_1(V_e-V_{mx}) + \frac{P_1 V_e{}^k}{1-k}\left[V^{1-k}\right]_{V_e}^{V_m} \tag{4}$$

Evaluating the definate integral gives the result

$$W_{com,c}= P_1(V_e-V_{mx}) + \frac{P_1 V_e}{k-1}\left(1- \frac{V_e}{V_m}^{k-1}\right) \tag{5}$$

By similar analysis, the work in each of the three other chambers is found to be

$$W_{exp,c}= \frac{P_3V_m}{k-1}\left[1-\left(\frac{V_m}{V_e}\right)^{k-1}\right]+ P_1(V_{mx}-V_e) \tag{6}$$

$$W_{com,p}= \frac{P_aV_{mxp}}{k-1}\left[1-\left(\frac{V_{mxp}}{V_{ep}}\right)^{k-1}\right]+ P_a(V_{mp}-V_{ep}) \tag{7}$$

$$W_{exp,p}= P_a(V_{mxp}-V_{mp}) \tag{8}$$

In equations (5) and (6), it is desirable to express $W_{exp,c}$ and $W_{com,c}$ in terms of the known parameters. These are P_a, pump inlet pressure, assumed equal to ambient; T_a, pump inlet temperature, also assumed equal to ambient; T_s, temperature rise during stoichiometric combustion; t, fuel-air mass ratio in the combustion chamber, expressed as a fraction of stoichiometric fuel-air mass ratio; and p, combustion chamber supercharge pressure ratio P_1/P_a. To so alter equation (5) requires only the use of the identity

$$P_1=P_ap \tag{9}$$

Equation (5) then becomes

$$W_{com,c}= P_ap\left\{V_e-V_{mx}+ \frac{V_e}{k-1}\left[1-\left(\frac{V_e}{V_m}\right)^{k-1}\right]\right\} \tag{10}$$

To solve in similar fashion for equation (6), it is necessary to solve for P_3 in terms of the desired parameters.

With perfect gas assumptions in a constant volume temperature rise, P/T remains constant. Therefore,

$$P_3 = P_2\left(\frac{T_2+T_b}{T_2}\right) \tag{11}$$

This is of course equivalent to

$$P_3 = P_2\left(1+ \frac{T_b}{T_2}\right) \tag{12}$$

In terms of the desired parameters,

$$P_3 = \frac{P_2}{P_1}\,\frac{P_1}{P_a}\,P_a\left(1+ \frac{T_b}{T_a}\,\frac{T_a}{T_1}\,\frac{T_1}{T_2}\right) \tag{13}$$

The term P_1/P_a is from equation (9) the combustion chamber supercharge pressure ratio p. Knowledge that the transition process from point 1 to point 2 is adiabatic gives the relations

$$\frac{P_2}{P_1} = \left(\frac{V_e}{V_m}\right)^k \tag{14}$$

and

$$\frac{T_1}{T_2} = \left(\frac{V_m}{V_e}\right)^k \tag{15}$$

If the supercharge compression is also taken as an adiabatic process,

$$\frac{T_a}{T_1} = p^{\frac{1-k}{k}} \tag{16}$$

Knowing the fuel heat content H_c and the specific heat of the fuel-air mixture, C_p, allows the calculation of the combustion chamber temperature rise during stoichiometric combustion,

$$T_s = \frac{H_c}{C_p} n_{gas} \qquad (17)$$

Defining the variable s as equal to the ratio T_s/T_a gives the relation

$$s = \frac{H_c n_{gas}}{C_p T_a} \qquad (18)$$

The actual temperature rise with nonstoichiometric conditions should be proportional to the fraction of stoichiometric fuel-air mixture injected, or

$$\frac{T_b}{T_s} = t \qquad (19)$$

Equations (17), (18), and (19) can now be combined to give an expression for T_b/T_a in terms of known parameters,

$$\frac{T_b}{T_a} = st \qquad (20)$$

Substituion of equations (9), (14), (15), (16), and (19) into equation (13) gives the desired relation,

$$P_3 = P_a\left[p\left(\frac{V_e}{V_m}\right)^k + stp^{\frac{1}{k}}\left(\frac{V_e}{V_m}\right)\right] \qquad (21)$$

Finally, substitution of (9) and (21) into equation (6) gives

$$W_{exp,c}=\frac{P_aV_m}{k-1}\left[p\left(\frac{V_e}{V_m}\right)^k+stp^{\frac{1}{k}}\frac{V_e}{V_m}\right]\left[1-\left(\frac{V_m}{V_e}\right)^{k-1}\right]+$$

$$P_ap(V_{mx}-V_e) \qquad (22)$$

or, multiplying out the binomials,

$$W_{exp,c}=\frac{P_aV_m}{k-1}\left[p\left(\frac{V_e}{V_m}\right)^k+stp^{\frac{1}{k}}\frac{V_e}{V_m}-p\frac{V_e}{V_m}-stp^{\frac{1}{k}}\left(\frac{V_e}{V_m}\right)^{2-k}\right]+$$

$$P_ap(V_{mx}-V_e) \qquad (23)$$

Making use of the expression

$$V_m=V_e\frac{V_m}{V_e} \qquad (24)$$

in equation (23) in order to simplify the bracketed term, the combination of resulting terms gives

$$W_{exp,c}=\frac{P_aV_e}{k-1}\left[p\left(\frac{V_e}{V_m}\right)^{k-1}-stp^{\frac{1}{k}}\left(\frac{V_e}{V_m}\right)^{1-k}+(stp^{\frac{1}{k}}-p)\right]+$$

$$P_ap(V_{mx}-V_e) \qquad (25)$$

There now exists in equations (7), (8), (10), and (25) expressions for the work produced in each chamber of the engine during a system half-cycle; that is, from piston rest at one end of the engine through acceleration and deceleration of the piston to rest at the other end of the engine. These four quantities represent work input to the piston. Since no external mechanical work is extracted from the piston, and piston-cylinder wall friction is assumed to be zero, the symmetry of the engine dictates an equilibrium cycle only if the net half-cycle work is equal to zero. This can be expressed as

$$W_{exp,c} + W_{com,c} + W_{exp,p} + W_{com,p} = 0 \qquad (26)$$

Substituting equations (7), (8), (10), and (25) into (26) results in the expression,

$$\frac{P_aV_e}{k-1}\left[p\left(\frac{V_e}{V_m}\right)^{k-1} - stp^{\frac{1}{k}}\left(\frac{V_e}{V_m}\right)^{1-k} + stp^{\frac{1}{k}} - p\right] + P_a p(V_{mx}-V_e)$$

$$+\frac{P_aV_{mxp}}{k-1}\left[1-\left(\frac{V_{mxp}}{V_{ep}}\right)^{k-1}\right] + P_a(V_{mp}-V_{ep}) + P_a p(V_e-V_{mx})$$

$$+\frac{P_a pV_e}{k-1}\left[1-\left(\frac{V_e}{V_m}\right)^{k-1}\right] + P_a(V_{mxp}-V_{mp}) = 0 \qquad (27)$$

Subtracting out identities gives

$$\frac{P_aV_e}{k-1}\, p^{\frac{1}{k}}st\left[1-\left(\frac{V_m}{V_e}\right)^{k-1}\right] + P_a(V_{mxp}-V_{ep})$$

$$+\frac{P_aV_{mxp}}{k-1}\left[1-\left(\frac{V_{mxp}}{V_{ep}}\right)^{k-1}\right] = 0 \qquad (28)$$

Simplifying and combining terms gives the desired final form of the equation,

$$stp^{\frac{1}{k}}\, V_e\left[1-\left(\frac{V_m}{V_e}\right)^{k-1}\right] + V_{ep}\left[k\frac{V_{mxp}}{V_{ep}} - \left(\frac{V_{mxp}}{V_{ep}}\right)^{k} + 1 - k\right] = 0 \qquad (29)$$

It should be emphasized that equation (29) must be satisfied in order for a system cycle to exist in equilibrium. If the value of the expression is less than zero, any oscillation will converge to zero; if it is greater than zero, the positive net work produced on each stroke will create a divergent piston cycle. Therefore, under the stipulation that the system exists at equilibrium, equation (29) gives one known relation in terms of four unknown variables.

Looking at the engine model depicted in figure 5, it seems clear that at one end of the stroke, the combination of pump chamber minimum and maximum volumes V_{mp} and V_{mxp} represents the total pump effective volume. This geometric condition is given by

$$V_{mxp} + V_{mp} = X_p A_p \qquad (30)$$

Also from the geometry of the engine model, it can be seen that in general

$$X_m + X_{mxp} + X_L = X_c + X_p \qquad (31)$$

If an infinite compression ratio existed for the pump chamber, the maximum compression in the combustion chamber would be determined by the difference between X_c and X_L. Choosing the value r to represent the maximum permitted combustion chamber compression ratio allows a reduction of variables by using the resulting equation,

$$X_c = X_L + \frac{X_e}{r} \qquad (32)$$

This equation in combination with equations (30) and (31) above results in a set of two further geometric constraints,

$$\frac{V_m}{A_c} = \frac{V_{mp}}{A_p} + \frac{X_e}{r} \tag{33}$$

$$\frac{V_{mx}}{A_c} = \frac{V_{mxp}}{A_p} + \frac{X_e}{r} \tag{34}$$

In order to estimate the mean half-cycle piston travel time, it is necessary to know the total unidirectional force which may act on the piston throughout a stroke. The unbalanced work is equal to

$$W = W_{exp,c} + W_{exp,p} \tag{35}$$

or, in equivalent form,

$$W = \left| W_{com,c} + W_{com,p} \right| \tag{36}$$

Choosing for convenience to use equation (36), the resulting expanded equation is

$$W = P_a p \left\{ V_{mx} - V_e + \frac{V_e}{k-1}\left[\left(\frac{V_m}{V_e}\right)^{1-k} - 1\right]\right\} + P_a \left\{ V_{ep} - V_{mp} + \frac{V_{mxp}}{k-1}\left[\left(\frac{V_{mxp}}{V_{ep}}\right)^{k-1} - 1\right]\right\} \tag{37}$$

It is now necessary to find an empirical relation to couple the mass of the piston with the various engine parameters. Due to its larger size, it may be stipulated that to first order, the piston mass depends only on the pump chamber characteristics. As a first order approach, it will be assumed that the piston mass will vary as

$$M_{pt} = \rho_{pt} X_p A_p \tag{38}$$

where ρ_{pt} is determined empirically from deriving piston volumes during a preliminary design phase, and applying the appropriate material densities to approximate piston weight.

The actual piston travel length during a half-cycle is equal to

$$L = \frac{V_{mxp} - V_{mp}}{A_p} \tag{39}$$

or, in equivalent form,

$$L = \frac{V_{mx} - V_m}{A_c} \tag{40}$$

Work is defined as a force integrated over the distance over which it is applied. Dividing this by the mass acted upon gives a mean velocity squared. From this, the half-cycle period is

$$Q = L\left(\frac{M_{pt}}{W}\right)^{\frac{1}{2}} \tag{41}$$

If the pump draws in air at standard atmospheric ambient conditions, and expands to the same conditions during the exhaust phase, the mass of pump air expelled is simply ambient density times the volume displaced, or

$$M_{o,p} = \rho_a (V_{mxp} - V_{ep}) \tag{42}$$

Assuming a nearly constant piston velocity, exhaust will occur during the fraction of the half-cycle proportional to the ratio of exhaust nozzle diameter to total stroke length, or

$$\dot{M}_p = \frac{M_{o,p}}{Q} \frac{D_{t,p} A_p}{V_{mxp} - V_{mp}} \tag{42}$$

By standard relation, mass flow is also equal to

$$\dot{M}_p = \frac{P_{o,p} A_{t,p}}{C_p^*} \tag{44}$$

The value of pump chamber stagnation pressure $P_{o,p}$ drops during exhaust from its peak initial value, found by the adiabatic compression relations for a perfect gas, to the ambient atmospheric pressure, P_a. Although chamber pressure in such a process generally follows an exponential decay law, by assuming that the characteristic process time is extremely short, the decay may be considered linear, and an average value taken as

$$P_{o,p} = \frac{P_a}{2} \left[\left(\frac{V_{mxp}}{V_{ep}} \right)^k + 1 \right] \tag{45}$$

In a similar manner, the average value of chamber stagnation temperature is found to be

$$T_{o,p} = \frac{T_a}{2} \left[\left(\frac{V_{mxp}}{V_{ep}} \right)^{k-1} + 1 \right] \tag{46}$$

The value C_p^* is the characteristic velocity of the fluid, and is defined as

$$C^*=\left[\frac{1}{k}\left(\frac{k+1}{2}\right)^{\frac{k+1}{k-1}} RT_o\right]^{\frac{1}{2}} \tag{47}$$

Substituting in the average chamber stagnation temperature found in equation (46), and using the perfect gas relation for speed of sound of ambient air,

$$A_{o,a}=(kRT_a)^{\frac{1}{2}} \tag{48}$$

the characteristic velocity may be found to be

$$C_p^* = gA_{o,a}\left(\frac{T_{o,p}}{T_a}\right)^{\frac{1}{2}} \tag{49}$$

where

$$g = \frac{1}{k}\left(\frac{k+1}{2}\right)^{\frac{k+1}{2(k-1)}} \tag{50}$$

Setting equation (43) equal to (44) and solving for $D_{t,p}$ gives the optimum pump chamber nozzle throat diameter,

$$D_{t,p}= \frac{gA_{o,a}M_{o,p}A_p}{\pi QP_{o,p}(V_{mxp}-V_{mp})}\left(\frac{T_{o,p}}{T_a}\right)^{\frac{1}{2}} \tag{51}$$

The standard equation for nozzle exhaust velocity is

$$U_e=\left\{2C_pT_o\left[1-\left(\frac{P_a}{P_o}\right)^{\frac{k-1}{k}}\right]\right\}^{\frac{1}{2}} \tag{52}$$

Using equations (45), (46), and (48), along with the perfect gas relation

$$C_p = \frac{k}{k-1} R \tag{53}$$

the final value for pump exhaust velocity is found to be

$$U_{e,p} = A_{o,a}\left\{\frac{2}{k-1}\,\frac{T_{o,p}}{T_a}\left[1-\left(\frac{P_{o,p}}{P_a}\right)^{\frac{1-k}{k}}\right]\right\}^{\frac{1}{2}} \tag{54}$$

Thrust produced by the pump is equal to the mass flow rate times the exhaust velocity, or

$$F_p = \frac{M_{o,p}U_{e,p}}{Q} \tag{55}$$

Usable thrust is also available by expansion of the combustion reaction products through nozzles to produce thrust. The mass which is available is the volume of air trapped when the exhaust port closes times the density, or

$$M_{o,c} = \rho_a p^{\frac{1}{k}} V_e \tag{56}$$

The average chamber stagnation pressure in the pump chamber is equal to

$$P_{o,c} = \tfrac{1}{2}(P_4 + P_1) \tag{57}$$

Using the adiabatic relation

$$\frac{P_4}{P_3} = \left(\frac{V_m}{V_e}\right)^k \tag{58}$$

and equations (9) and (21), the relation for combustion chamber pressure becomes

$$P_{o,c} = P_a \; p + \left[\frac{st}{2} p^{\frac{1}{k}} \left(\frac{V_m}{V_e} \right)^{k-1} \right] \tag{59}$$

Similarly, the average combustion chamber stagnation temperature becomes

$$T_{o,c} = T_a \left[p^{\frac{k-1}{k}} + \tfrac{1}{2} st \left(\frac{V_m}{V_e} \right)^{k-1} \right] \tag{60}$$

In the combustion chamber, the exhaust port is uncovered from V_e until the piston reaches bottom dead center at V_{mx} and returns to V_e. The mass flow rate required must then be

$$\dot{M}_{o,c} = \frac{2M_{o,c}}{Q} \frac{V_{mx} - V_e}{V_{mx} - V_m} \tag{61}$$

As before, this is equal to

$$\dot{M}_c = \frac{P_{o,c} A_{t,c}}{C_c^*} \tag{62}$$

Setting the two previous equations equal to each other and solving for the optimum combustion chamber throat diameter gives

$$D_{t,c} = \left[\frac{M_{o,c}}{Q} \frac{8gA_{o,a}}{\pi \; P_{o,c}} \left(\frac{T_{o,c}}{T_a} \right)^{\frac{1}{2}} \frac{V_{mx} - V_e}{V_{mx} - V_m} \right]^{\frac{1}{2}} \tag{63}$$

The combustion chamber exhaust velocity is found to be

$$U_{e,c} = A_{o,a}\left\{\frac{2}{k-1}\,\frac{T_{o,c}}{T_a}\left[1-\left(\frac{P_{o,c}}{P_a}\right)^{\frac{1-k}{k}}\right]\right\}^{\frac{1}{2}} \qquad (64)$$

And, in similar form as for the pump chamber, the thrust produced by the combustion chamber is equal to

$$F_c = \frac{M_{o,c}U_{e,c}}{Q} \qquad (65)$$

The total thrust produced by the engine is, by inspection,

$$F = F_c + F_p \qquad (66)$$

The engine bypass ratio is defined to be the mass flow through the pump chamber divided by the mass flow through the combustion chamber, or

$$bpr = \frac{M_{o,p}}{M_{o,c}} \qquad (67)$$

Specific fuel consumption is defined as the mass flow rate of fuel divided by the thrust produced. During each half-cycle, the mass of fuel injected is simply the stoichiometric fuel-air mass ratio times the throttle setting, referenced to stoichiometric conditions, times the total mass of air present in the combustion chamber. Dividing this quantity by the thrust gives the result

$$SFC = \frac{tV_e n_{gas}}{QF}\,\rho_a p^{\frac{1}{k}} \qquad (68)$$

2.3 Parameterization and Nondimensionalization

In order to generalize the engine analysis so that it applies to all engine sizes, it is desirable to express the basic equations in terms of nondimensional engine parameters; p, combustion chamber supercharge pressure ratio, t, throttle setting in percent of stoichiometric mixture ratio, stoichiometric temperature ratio s, and other parameters which have not yet been defined. These include length ratios x_p and x_{ep}, area ratios a_c and a_p, and density ratio e. The definitions of the parameters are

$$a_c = \frac{A_c}{X_e^2} \tag{69}$$

$$a_p = \frac{A_p}{X_e^3} \tag{70}$$

$$x_p = \frac{X_p}{X_e} \tag{71}$$

$$x_{ep} = \frac{X_{ep}}{X_e} \tag{72}$$

$$e = \frac{\rho_{pt}}{\rho_a} \tag{73}$$

Throughout the work equilibrium equation, the variables V_m and V_{mxp} appear as ratios only of their respective exhaust volumes. Therefore, for simplicity,

$$v_m = \frac{V_m}{V_e} \tag{74}$$

$$v_{mxp} = \frac{V_{mxp}}{V_{ep}} \tag{75}$$

Dividing through equation (29) by X_e^3 gives, after simplification, the nondimensional form of the work equilibrium equation,

$$p^{\frac{1}{k}} a_c ts(1-v_m{}^{k-1}) + x_{ep} a_p (kv_{mxp} - v_{mxp}{}^k + 1 - k) = 0 \tag{76}$$

Equation (30), which uses continuity of pump chamber effective volume, becomes

$$v_{mxp} + v_{mp} = \frac{x_p}{x_{ep}} \tag{77}$$

The geometric constraints, equations (33) and (34), are in dimensionless form

$$v_m = v_{mp} x_{ep} + \frac{1}{r} \tag{78}$$

$$v_{mx} = v_{mxp} x_{ep} + \frac{1}{r} \tag{79}$$

Equations (76) to (79) now represent a set of four equations, with four unknowns. For any given set of engine geometric and thermodynamic parameters, these equations will give the maximum and minimum volumes of the pump and combustion pistons in an equilibrium cycle. For consistency with v_m and v_{mxp}, the other two volume ratios are defined as

$$v_{mx} = \frac{V_{mx}}{V_e} \tag{80}$$

$$v_{mp} = \frac{V_{mp}}{V_e} \tag{81}$$

The cycle forcing work W is nondimensionalized by dividing through by $P_a X_e^{\,3}$, to give

$$w = \frac{W}{P_a V_e^{\,3}} = pa_c\left(v_{mx} - \frac{k}{k-1} + \frac{1}{k-1}\, v_m^{\,1-k}\right) +$$

$$+ a_p x_{ep}\left[1 - v_{mp} + \frac{1}{k-1}(v_{mxp}^{\,k} - v_{mxp})\right] \tag{82}$$

Piston mass is made dimensionless by dividing through by $\rho_a X_e^3$, so

$$m_{pt} = \frac{M_{pt}}{\rho_a X_e^{\,3}} = \frac{\rho_{pt}}{\rho_a}\, x_p a_p \tag{83}$$

or, in more convenient form,

$$m_{pt} = \frac{M_{pt}}{\rho_a e X_e^{\,3}} = x_p a_p \tag{84}$$

The piston travel length parameter becomes

$$l = \frac{L}{X_e} = (v_{mxp} - v_{mp}) x_{ep} \tag{85}$$

Direct substitution of equations (82), (84), and (85) into (41) gives

$$q = \frac{Q}{X_e}\left(\frac{P_a}{\rho_a e}\right)^{\frac{1}{2}} = l\left(\frac{m_{pt}}{w}\right)^{\frac{1}{2}} \tag{86}$$

The exhaust mass are nondimensionalized as in equation (83) to find

$$m_{o,p}=\frac{M_{o,p}}{\rho_a X_e{}^3}=(v_{mxp}-1)a_p x_{ep} \tag{87}$$

$$m_{o,c}=\frac{M_{o,c}}{\rho_a X_e{}^3}=p^{\frac{1}{k}}a_c \tag{88}$$

Pressures are made nondimensional by dividing through by P_a, which gives the relations

$$p_{o,p}=\frac{P_{o,p}}{P_a}=\tfrac{1}{2}(v_{mxp}{}^{k}+1) \tag{89}$$

$$p_{o,c}=\frac{P_{o,c}}{P_a}=p+\tfrac{1}{2}stp^{\frac{1}{k}}v_m{}^{k-1} \tag{90}$$

Similarly, temperatures are nondimensionalized by T_a,

$$t_{o,p}=\frac{T_{o,p}}{T_a}=\tfrac{1}{2}(v_{mxp}{}^{k-1}+1) \tag{91}$$

$$t_{o,c}=\frac{T_{o,c}}{T_a}=p^{\frac{k-1}{k}}+\tfrac{1}{2}stv_m{}^{k-1} \tag{92}$$

Substituting in the nondimensional form of the constituent equations allows the solution for the dimensionless nozzle throat diameters,

$$d_{t,p}=\frac{\pi D_{t,p}}{gA_{o,a}X_e}\left(\frac{eP_a}{a}\right)^{\frac{1}{2}}=\frac{m_{o,p}t_{o,p}{}^{\frac{1}{2}}}{qp_{o,p}(v_{mxp}-v_{mp})x_{ep}} \tag{93}$$

$$d_{t,c} = \frac{D_{t,c}}{X_e}\left(\frac{P_a}{\rho_a e}\right)^{1/4}\left(\frac{\pi}{8gA_{o,a}}\right)^{\frac{1}{2}} = \left(\frac{m_{o,c}}{qp_{o,c}}\,\frac{v_{mx}-1}{v_{mx}-v_m}\right)^{\frac{1}{2}} \qquad (94)$$

The exhaust velocities were nondimensionalized with the ambient speed of sound. It should be noted that the dimensionless form of the exhaust velocity is identically the exhaust Mach number in a perfect gas. The exhaust velocity equations become

$$u_{e,p} = \frac{U_{e,p}}{A_{o,a}} = \left[\frac{2}{k-1}\, t_{o,p}\left(1-p_{o,p}^{\frac{1-k}{k}}\right)\right]^{\frac{1}{2}} \qquad (95)$$

$$u_{e,c} = \frac{U_{e,c}}{A_{o,a}} = \left[\frac{2}{k-1}\, t_{o,c}\left(1-p_{o,c}^{\frac{1-k}{k}}\right)\right]^{\frac{1}{2}} \qquad (96)$$

The thrust equations become, in dimensionless form

$$f_c = \frac{F_c}{A_{o,a}X_e^2}\left(\frac{e}{\rho_a P_a}\right)^{\frac{1}{2}} = \frac{m_{o,c}u_{e,c}}{q} \qquad (97)$$

$$f_p = \frac{F_p}{A_{o,a}X_e^2}\left(\frac{e}{\rho_a P_a}\right)^{\frac{1}{2}} = \frac{m_{o,p}u_{e,p}}{q} \qquad (98)$$

$$f = f_c + f_p \qquad (99)$$

The specific fuel consumption is now

$$sfc = \frac{SFC}{n_{gas}} A_{o,a} = \frac{ta_c p^{\frac{1}{k}}}{fq} \qquad (100)$$

The bypass ratio is unchanged, but expressed in dimensionless form becomes

$$bpr = \frac{m_{o,p}}{m_{o,c}} \tag{101}$$

Another parameter of interest is the contribution of the combustion chamber to overall thrust. This factor is found by the equation

$$pfc = \frac{f_c}{f} \tag{102}$$

CHAPTER 3

RESULTS

3.1 Variational Analysis

Using the set of nondimensional equations derived in the last section, a preliminary study was performed to determine the variations in engine cycles and performance with changes in the chosen geometric and thermodynamic variables. The chosen baseline engine parameters for this study are

$$p = \frac{P_1}{P_a} = 1.0 \tag{103}$$

$$t = \frac{T_b}{T_s} = 1.0 \tag{104}$$

$$a_c = \frac{A_c}{X_e{}^2} = 1.0 \tag{105}$$

$$a_p = \frac{A_p}{X_e{}^2} = 4.0 \tag{106}$$

$$x_{ep} = \frac{X_{ep}}{X_e} = .25 \tag{107}$$

$$x_p = \frac{X_p}{X_e} = 2.0 \tag{108}$$

$$s = \frac{T_s}{T_a} = 10.0 \tag{109}$$

These figures were chosen on the basis of comparing favorably with comparable values for similar ratios in standard internal combustion engines, and also on the basis of trial analysis which showed that both cycle performance and engine performance fell within a range of interest. It should probably be explained that "cycle performance" refers to the parameters of the equilibrium engine cycle, such as compression ratio and cycle period, while "engine performance" refers to engine characteristics of interest, such as thrust and specific fuel consumption coefficients.

After the baseline parameters were arrived at, a single dimension variational analysis was performed, in which the values of one parameter were allowed to vary, while the other parameters were kept fixed to their baseline values. The results of this analysis are contained in figures 8 - 26.

Probably the most surprising result is the behavior of v_m with a change of parameters. For increasing supercharge ratios, or increasing temperature ratios which would correspond to increasing fuel flow, the compression fraction increases, or, alternatively, the compression ratio decreases. This would seem to be contrary to intuition gained from conventional internal combustion engines, where an increase in either or both of the aforementioned parameters results in an increase in power. However, since the piston is not constrained in its cycle by a connecting rod and crankshaft assembly, it must seek work equilibrium in order for a cycle to exist. Since increasing p or t results in an ability to extract more work from the combustion chamber at a given compression ratio, the engine must seek a lower compression ratio in order to re-establish equilibrium. Due to the configuration, and increase in v_m is directly proportional to a corresponding decrease in v_{mxp}. This results in a lower mass flow rate of air with an increase in fuel flow, and lower thrust compounds the increase in specific fuel consumption. This can clearly be seen in Figure 10, with the decrease in bypass ratio and increase in percentage of engine thrust produce by the combustion chambers, as the supercharge ratio increases. From this, unless thrust is an overriding critical item, it seems clear that the optimum choice of p and t would be the least values which allow a cycle to take place with reasonable compression ratios.

The value a_c most clearly corresponds in a standard internal combustion engine with the ratio of bore to stroke. As the distance from the combustion chamber exhaust port to the head increases with respect to the cylinder diameter, the thrust initially drops rapidly with the decrease in v_m, then increases again as the larger combustion chamber volume begins to produce higher percentages of thrust. However, this trend is followed by a similar increase in specific fuel consumption.

A change in a_p has the opposite effect, with an increase in thrust, decrease in specific fuel consumption, increase in bypass ratio, and drop in combustion chamber thrust percentage. This is to be expected, as a_p represents the area of the pump chamber, and its increase indicates the corresponding increase in available bypass volume.

There seems to be little latitude in choice of x_{ep}, as a small change makes a large difference in compression ratio. Since thrust follows this trend, it is best to keep x_{ep} at a minimum.

There is equally little latitude in x_p. This is a very strong corollary to compression ratio, and is picked on the basis of the other parameters.

From all of this, it might seem that the key to maximum engine performance would be to decrease t, a_c, and x_{ep}, and increase a_p and x_p. The value of p would depend on whether thrust or fuel consumption is the driving factor. Yet, all of these parameters also influence the compression ratio. This is probably the major departure from normal internal combustion engines, in that there is no mechanical constraint on compression ratio. The designer cannot pick a number to his of her own liking, and design a crankshaft and connecting rods to match. The value of v_m can only be influenced by choice of engine parameters. It must be within reasonable limits: too low, and the cycle efficiency of the combustion chamber will approach zero. If the compression ratio is too high, problems will arise from the onset of detonation, with the corresponding structural complications. For this reason, the equations were written with an additional constraint factor r, which is a limiting compression ratio. However, for this trend analysis, the value of 1/r was allowed to go to zero.

3.2 Prototype Flight Engine

The objective of the prototype flight engine design is to find if an engine can be designed from the preceding calculations which would be applicable to a small, single-seat personal airplane, on the order of a BD-5. Off-the-shelf components should be used as much as possible, to reduce construction costs and time, and improve reliablity.

The engine was sized by the decision to use Volkswagen pistons and cylinders for the combustion section of the engine. The cylinders are finned to dissipate heat, however, the Volkwagen engine is normally a four-stroke engine with intake and exhaust valves in the cylinder head; therefore the cylinder will have to be modified for use in a two-cycle ported engine.

The diameter of the Volkswagen piston is 85.5 mm. The length of the cylinder is 136 mm, however, since the section of the piston containing the rings must not travel outside of the cylinder, the maximum stroke length is 72 mm. Since thrust is scaled proportional to the square of the exhaust distance, it is desired to keep X_e as large as possible. For this reason, a_c was taken as equal to 1.5. In turn, X_e was found to be .203 feet.

Since the maximum piston travel is a constraint in the combustion chamber, x_p is no longer an independent variable. With a choice of maximum compression ratio equal to 12, x_p was found to be 1.048, giving a pump chamber effective length of .213 feet. The supercharge pressure ratio p was taken as 1, for simplicity; and t_t was taken as .85. The value of s was set equal to 10 on the basis of available heat in gasoline. From this point, an analysis was performed to determine values of a_p and x_{ep} which would provide a reasonable combustion cycle. These were found to be a_p=10 and x_{ep}=.165. These values resulted in a compression ratio of 10.3:1.

Finding a value of e=1000 from a previous design, the engine characteristics of the prototype engine were calculated, and are presented in table 1. Of special note is the thrust level of 109 pounds, thrust/weight ratio of approximately 4, and specific fuel consumption of .465 pounds of fuel per hour, per pound of thrust. Compared to the Sermel engine in the BD-5J, the dual mode free piston jet engine compares favorably in all aspects (T/W=4 compared to 3, SFC = .465 compared to 1.45) save one. That is, the dual mode free piston jet engine currently exists only on paper. But it does show great promise, even if these equations are only somewhat accurate.

CHAPTER 4

SUMMARY

It has been shown from a work equilibrium viewpoint that an equilibrium cycle does exist for the dual mode free piston jet engines. The results of the cycle analysis, together with the engine parameters, can and have been used to derive performance estimates for such an engine, and have been converted to non-dimensional form for use in engine optimization. With a given set of dimensions from a Volkswagen cylinder, a set of engine parameters was chosen to give reasonable performance, which was then analyzed.

It all comes down to the dichotomy between theory and reality. Assumptions have been made throughout, such as perfect gases, adiabatic compression, and no wall friction. None of these conditions exists in the real world. Yet, the results indicate that it is possible to build a prototype engine with a weight in the neighborhood of 25 pounds, a thrust level exceeding one hundred pounds, and specific fuel consumption below .5 pounds of fuel per hour, per pound of thrust. If these things can be achieved, the dual mode free piston jet engine represents a viable alternative in light aircraft powerplant selection. It only remains to build one and see.

FIGURE 1

ORIGINAL ENGINE CONFIGURATION

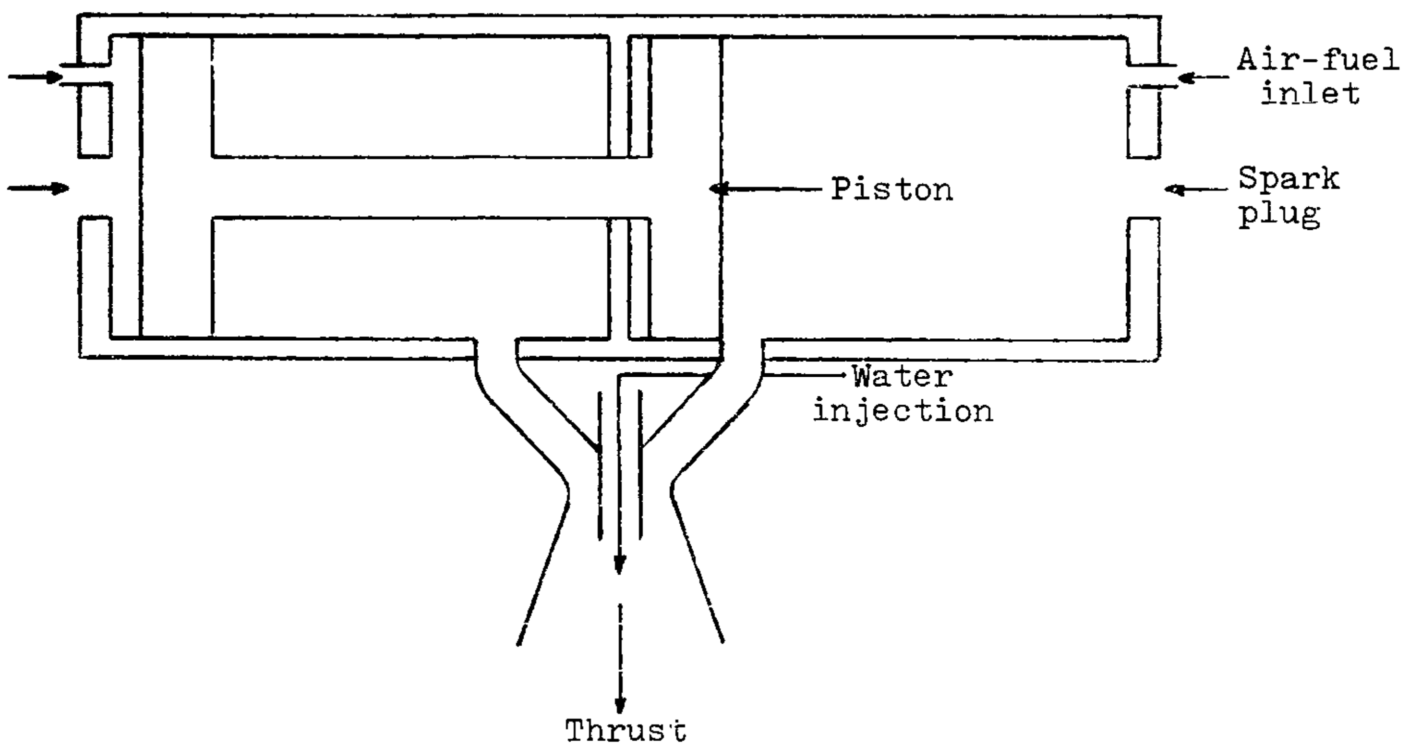

FIGURE 2

SKIRTED PISTON MODIFICATION

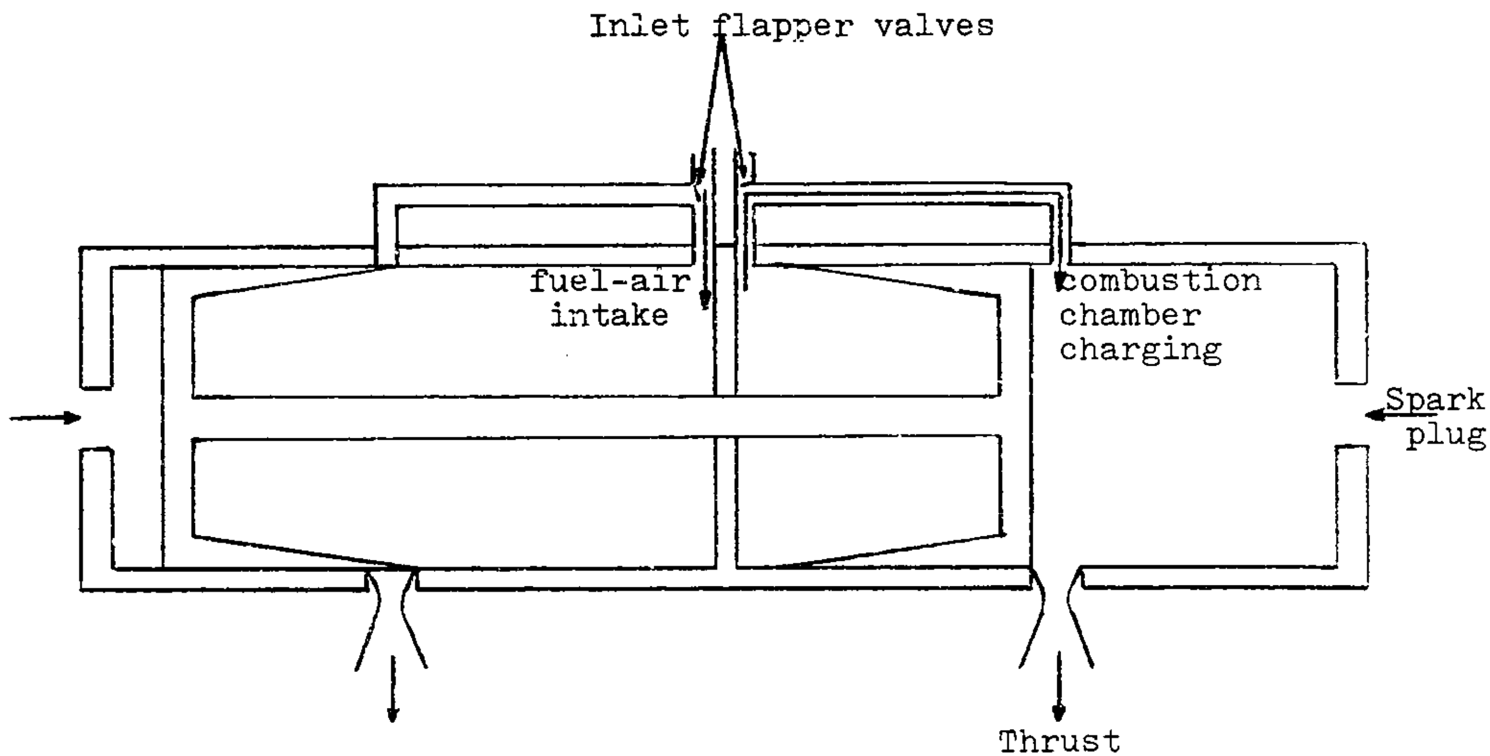

FIGURE 3

ASYMMETRIC DUAL MODE MODIFICATION

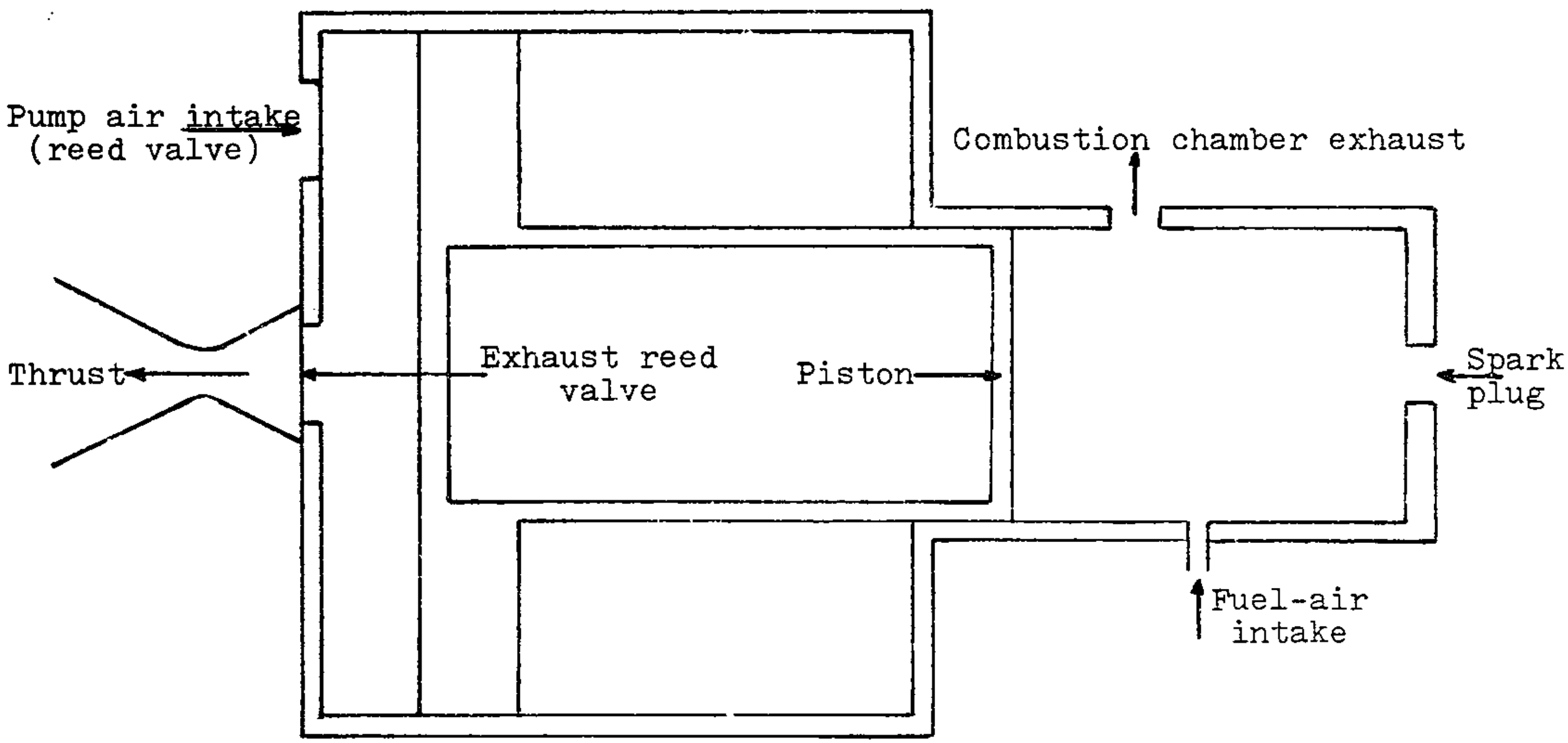

FIGURE 4

SYMMETRICAL PORTED DUAL MODE CONFIGURATION

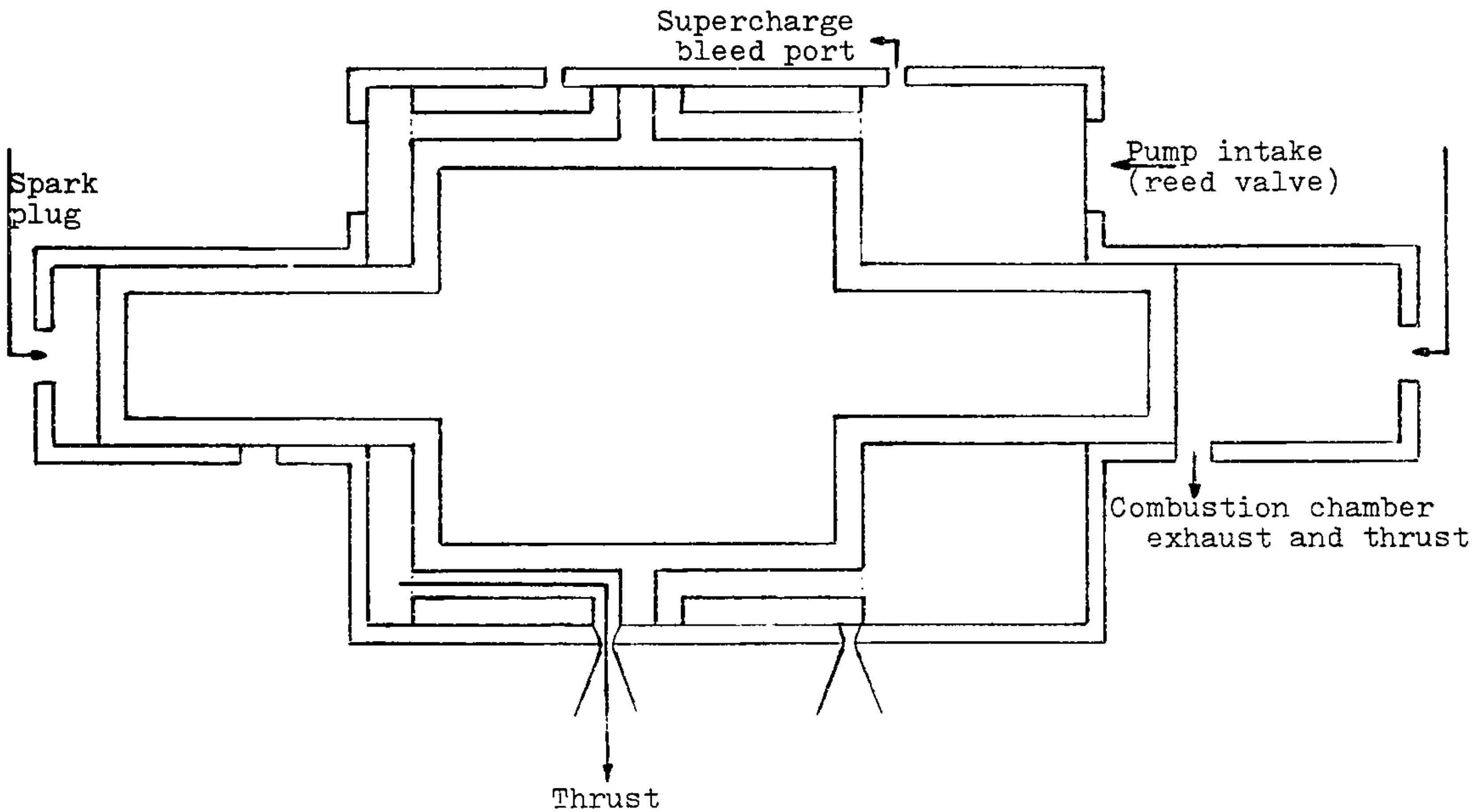

FIGURE 5

ENGINE MODEL

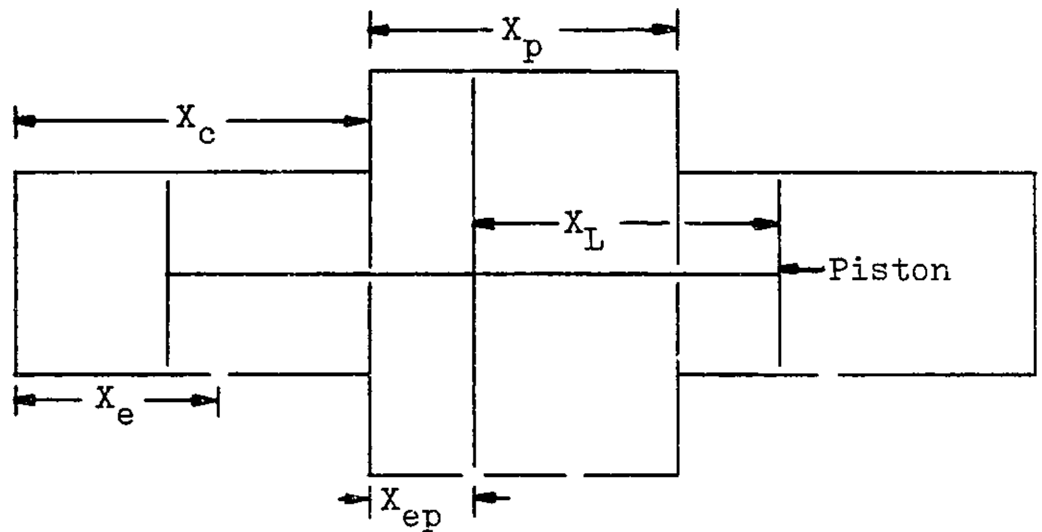

FIGURE 6

COMBUSTION CHAMBER CYCLE

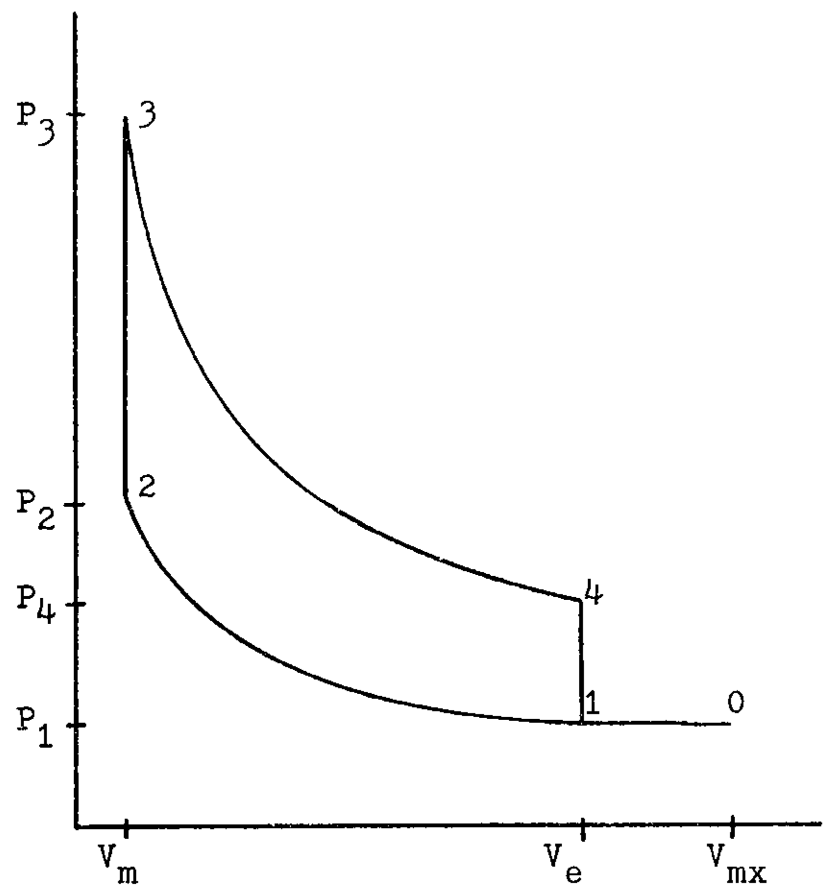

FIGURE 7

PUMP CHAMBER CYCLE

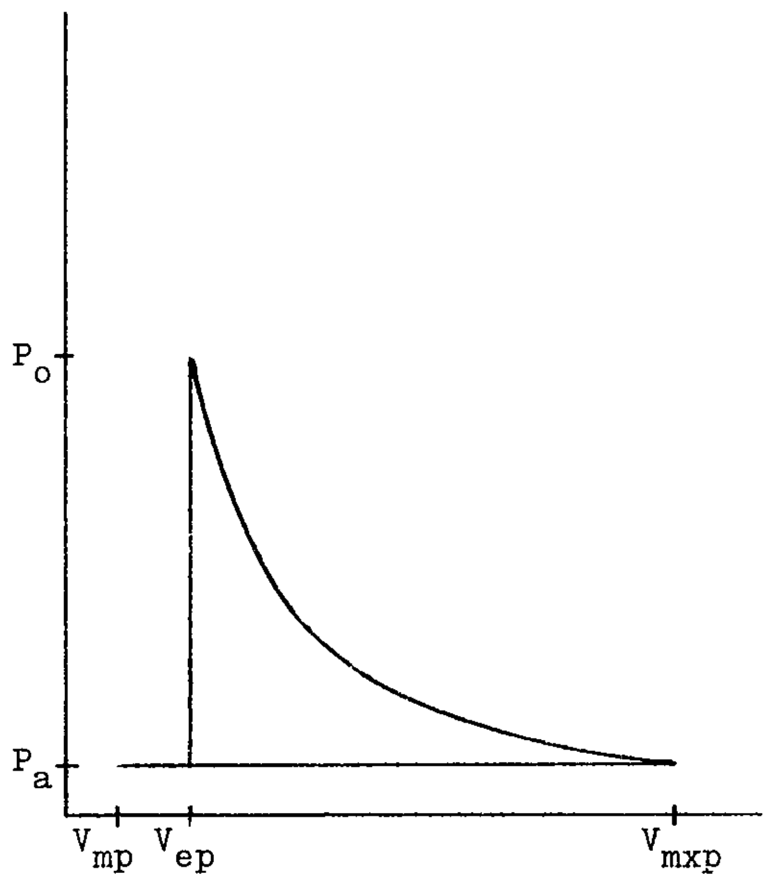

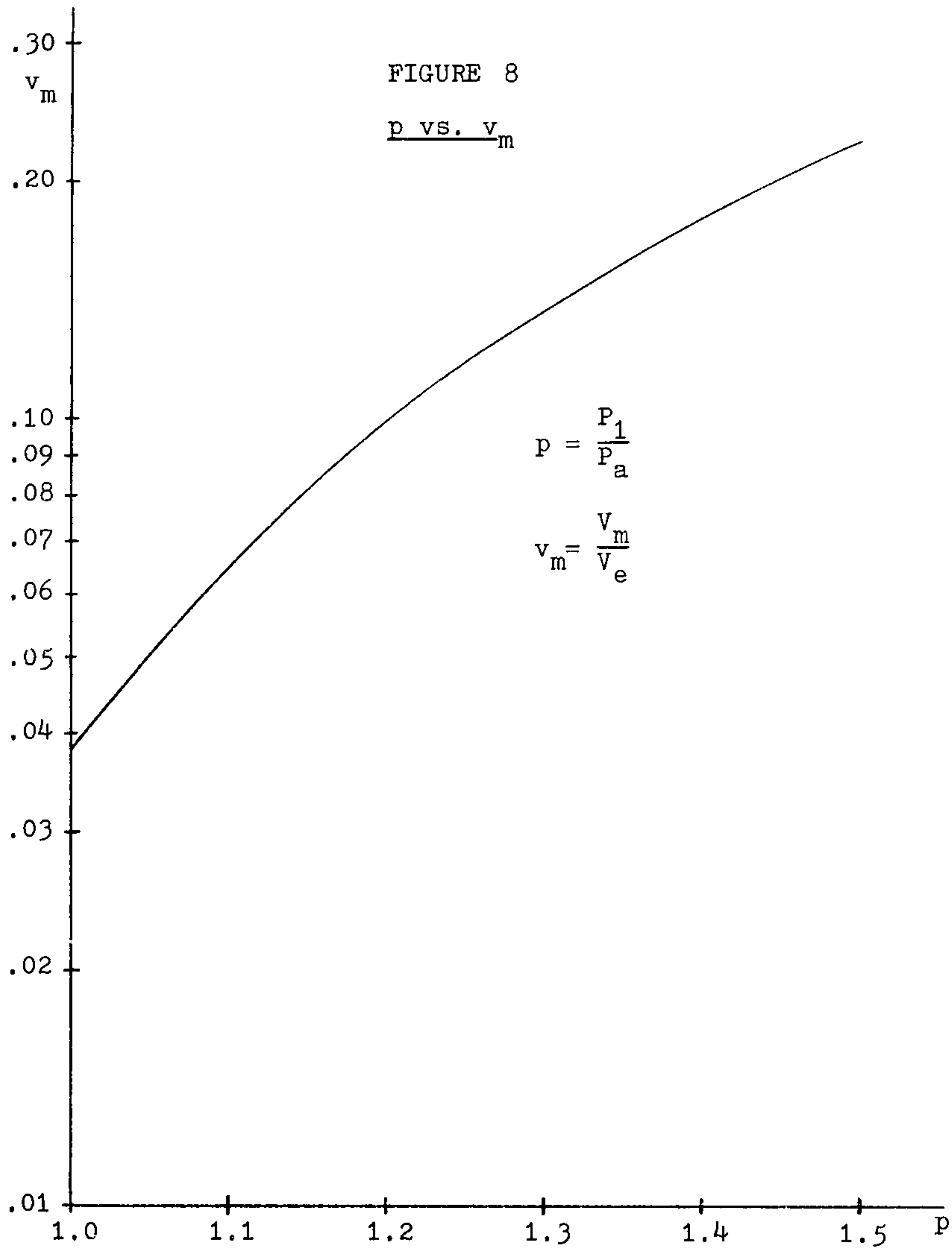

.30
v_m
FIGURE 8
p vs. v_m
.20
.10
.09
.08
.07
.06
.05
.04
.03
.02
.01
$p = \frac{P_1}{P_a}$
$v_m = \frac{V_m}{V_e}$
1.0
1.1
1.2
1.3
1.4
1.5
p

FIGURE 9

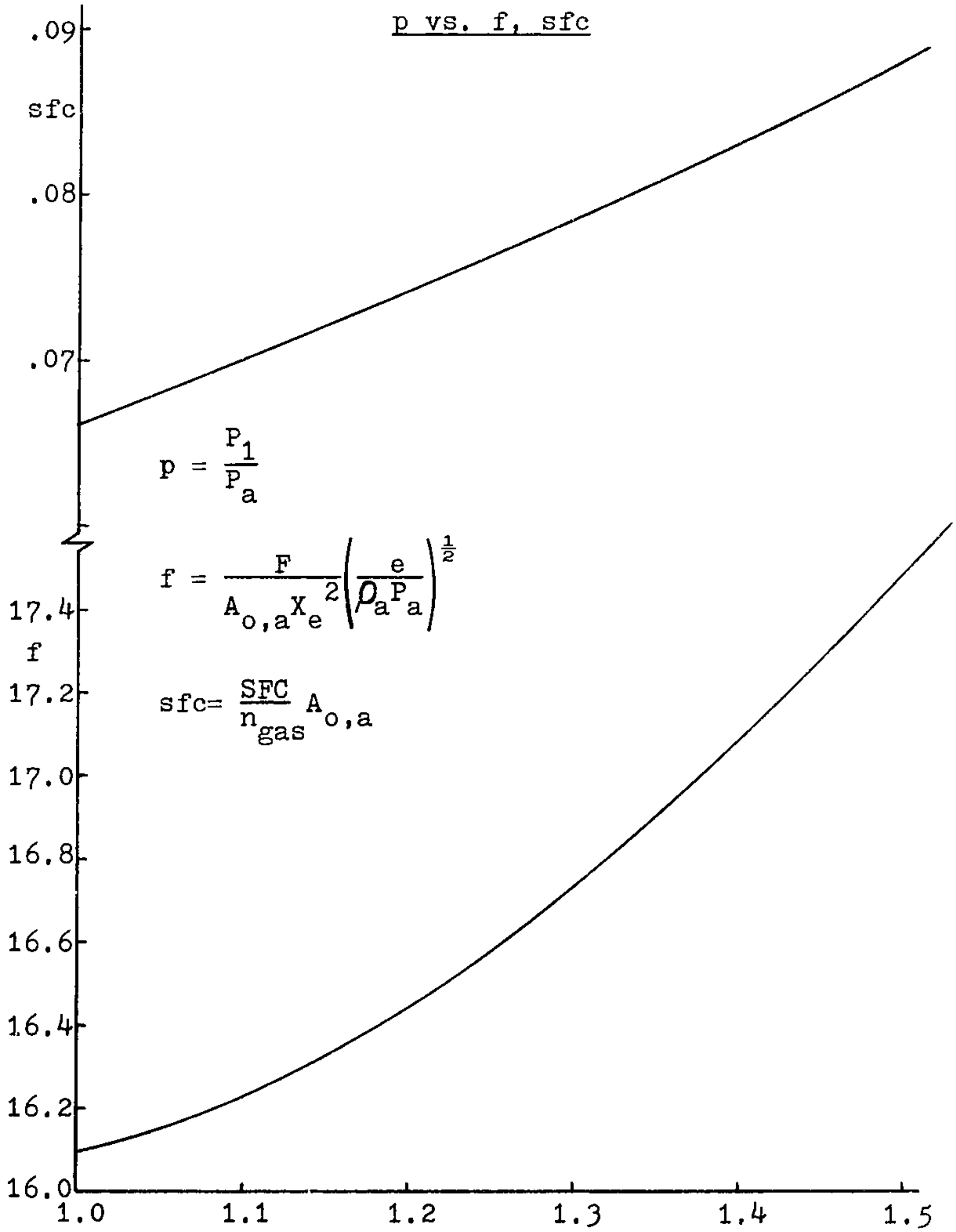
p vs. f, sfc
.09
sfc
.08
.07
$p = \frac{P_1}{P_a}$
$f = \frac{F}{A_{o,a} X_e^2} \left(\frac{e}{\rho_a P_a} \right)^{\frac{1}{2}}$
17.4
f
17.2
$sfc = \frac{SFC}{n_{gas}} A_{o,a}$
17.0
16.8
16.6
16.4
16.2
16.0
1.0
1.1
1.2
1.3
1.4
1.5

FIGURE 10

p vs. bpr, pfc

$p = \frac{P_1}{P_a}$ $bpr = \frac{M_{o,p}}{M_{o,c}}$ $pfc = \frac{F_c}{F}$

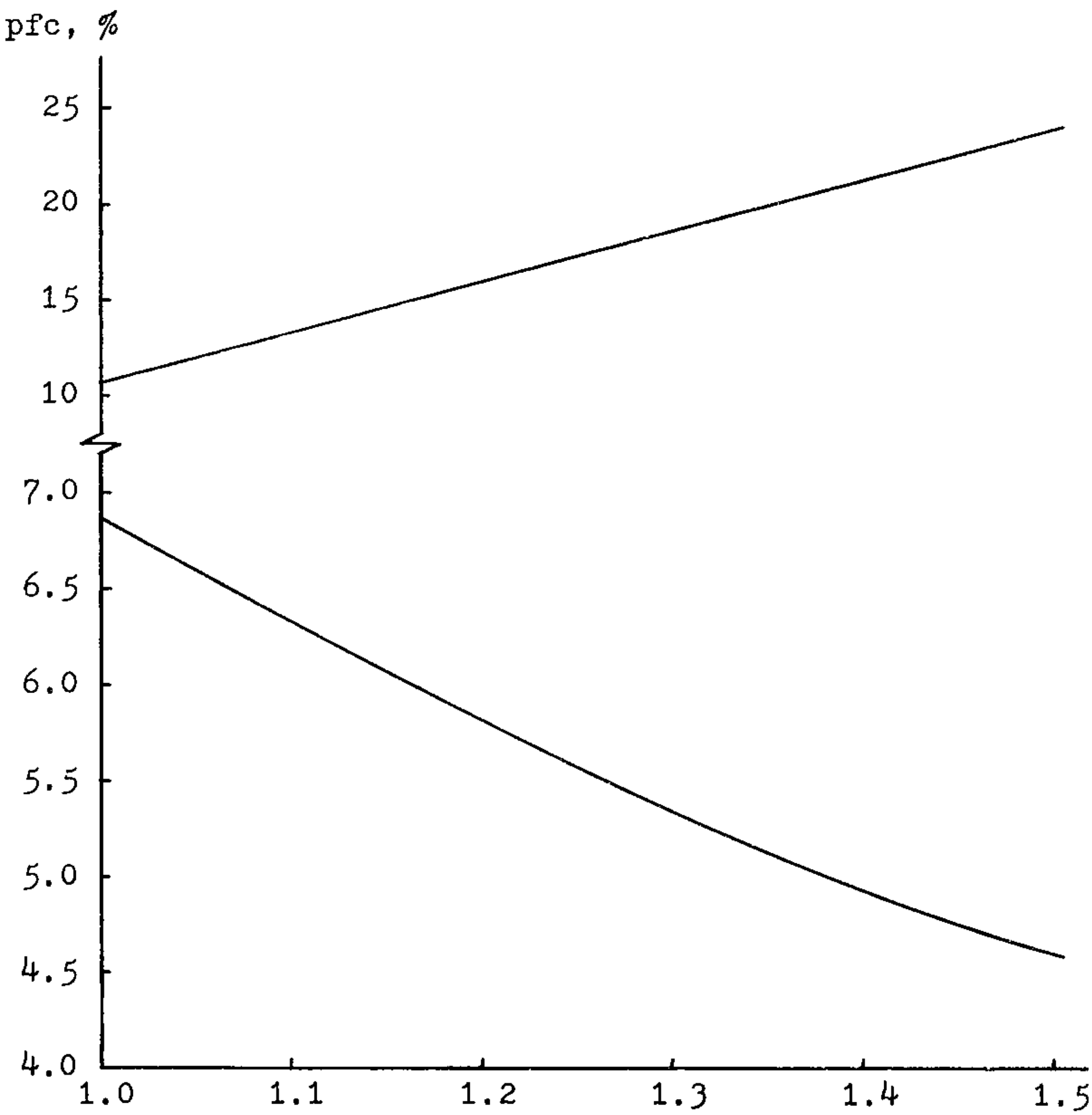

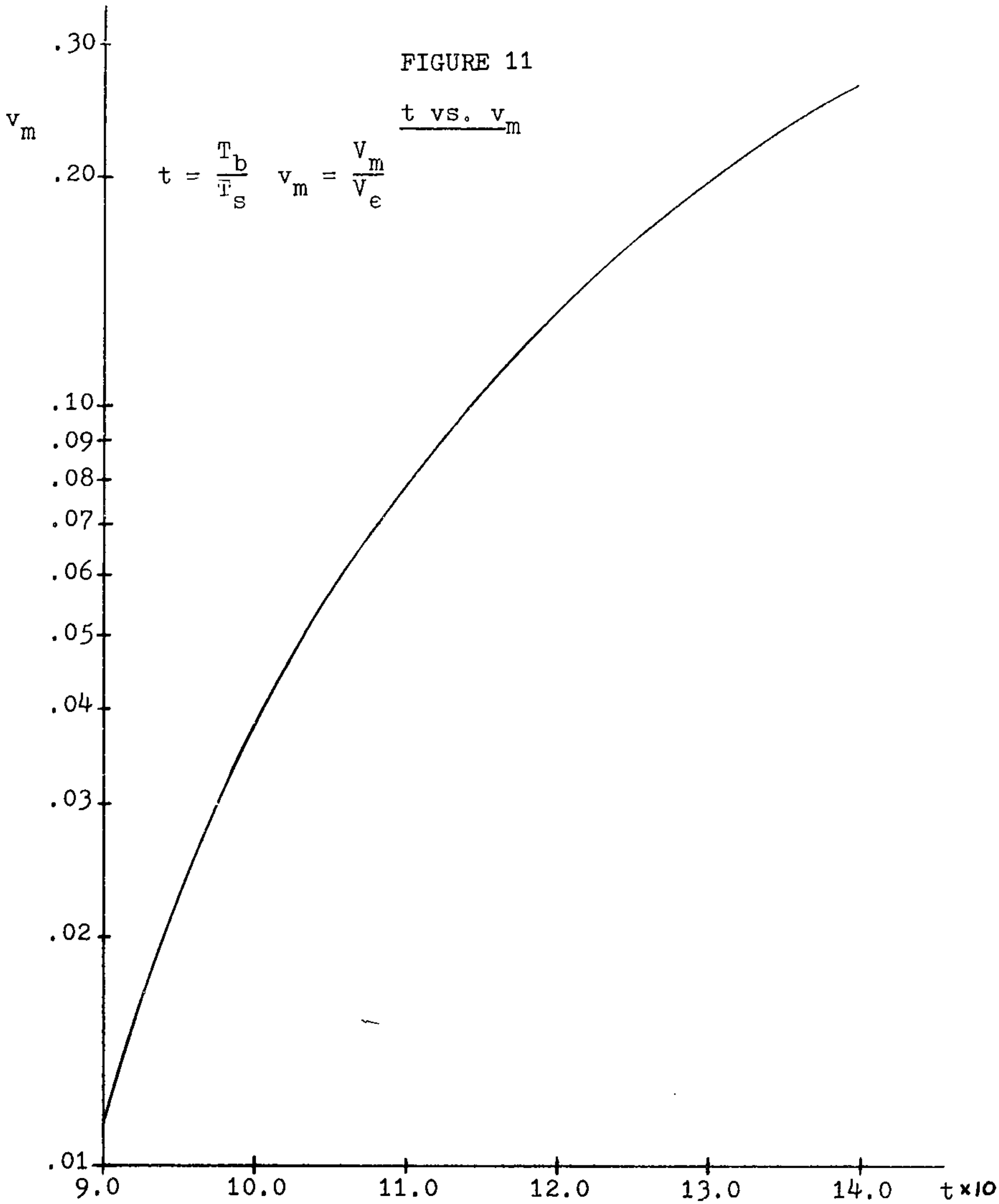

FIGURE 11
t vs. v_m
$t = \frac{T_b}{T_s}$ $v_m = \frac{V_m}{V_e}$
v_m
.30
.20
.10
.09
.08
.07
.06
.05
.04
.03
.02
.01
9.0
10.0
11.0
12.0
13.0
14.0
t ×10

FIGURE 12

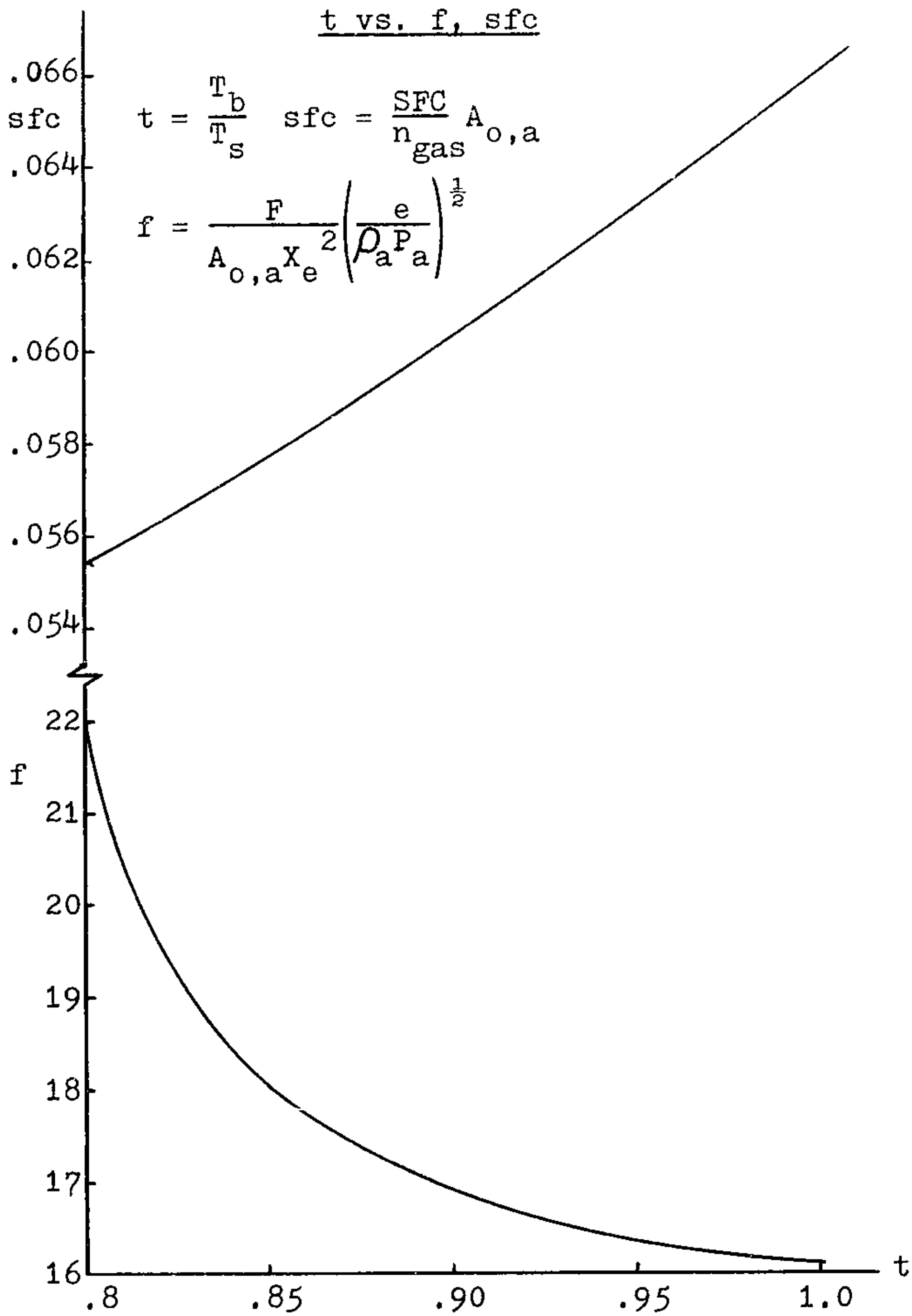
t vs. f, sfc
$t = \frac{T_b}{T_s}$ $sfc = \frac{SFC}{n_{gas}} A_{o,a}$
$f = \frac{F}{A_{o,a} X_e^2} \left(\frac{e}{\rho_a P_a} \right)^{\frac{1}{2}}$
sfc
.066
.064
.062
.060
.058
.056
.054
f
22
21
20
19
18
17
16
.8
.85
.90
.95
1.0
t

FIGURE 13

t vs. bpr, pfc

$t = \frac{T_b}{T_s}$ $bpr = \frac{M_{o,p}}{M_{o,c}}$ $pfc = \frac{F_c}{F}$

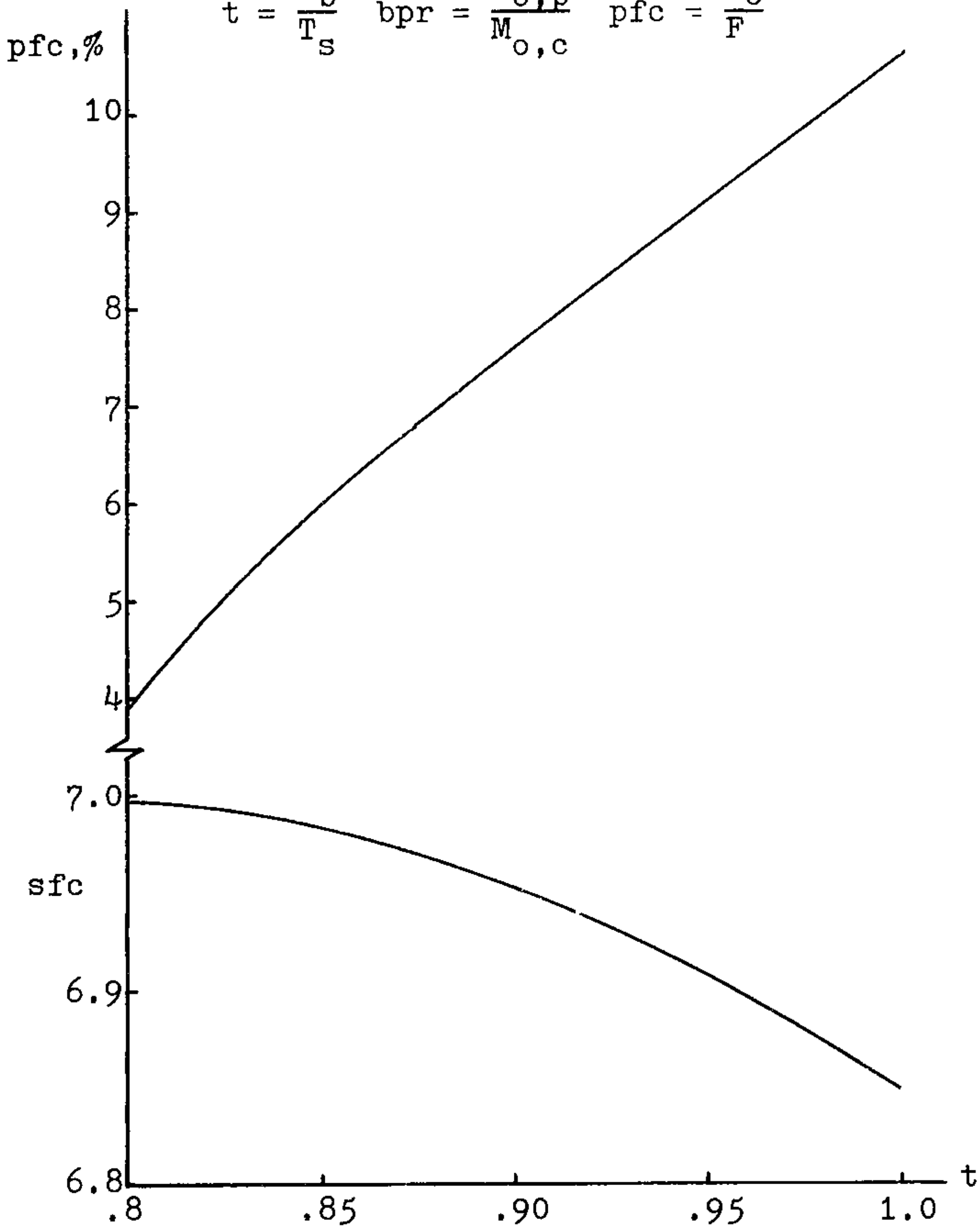

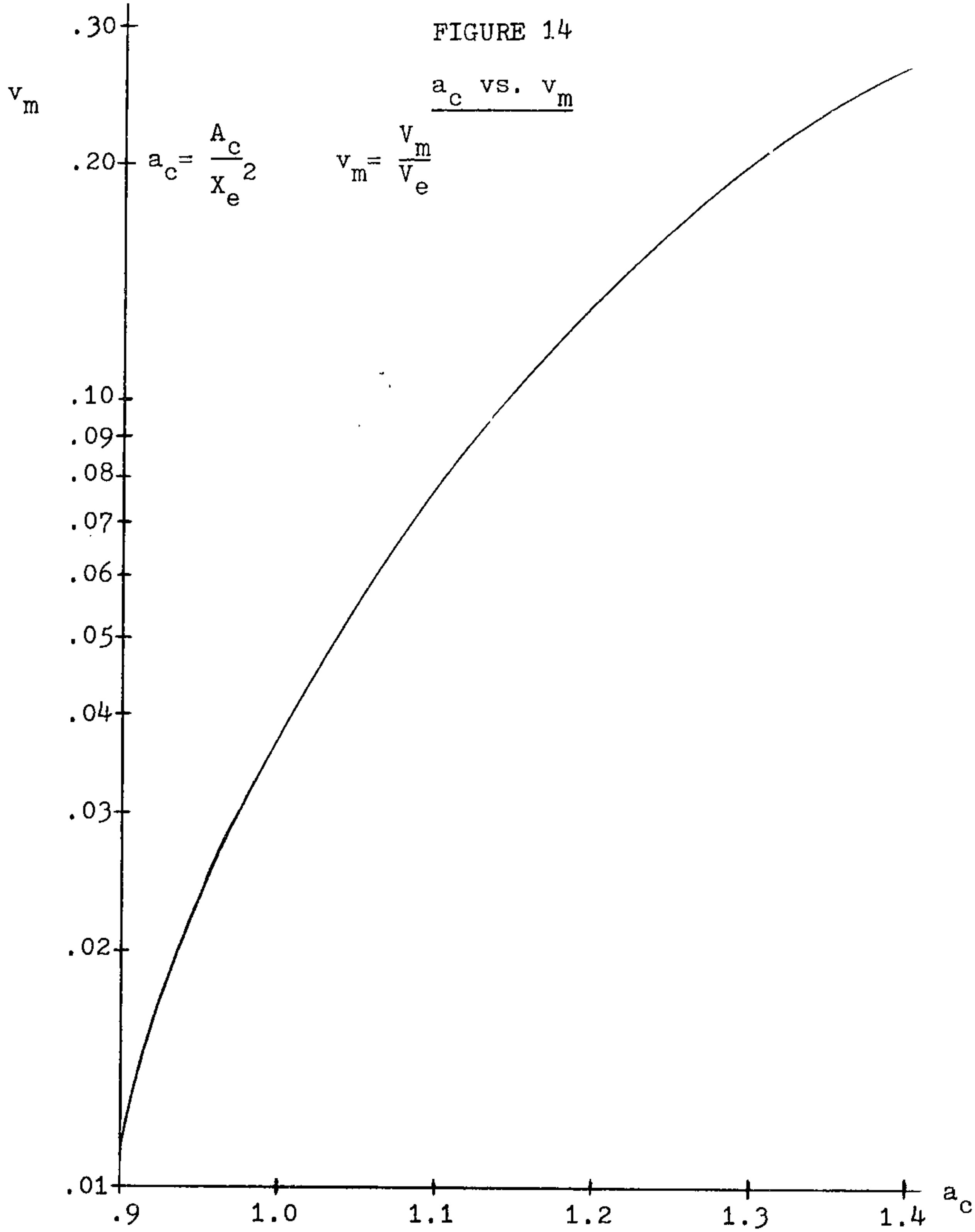
FIGURE 14
a_c vs. v_m
v_m
$a_c = \frac{A_c}{X_e^2}$
$v_m = \frac{V_m}{V_e}$
.30
.20
.10
.09
.08
.07
.06
.05
.04
.03
.02
.01
.9
1.0
1.1
1.2
1.3
1.4
a_c

FIGURE 15

<u>a_c vs. f, sfc</u>

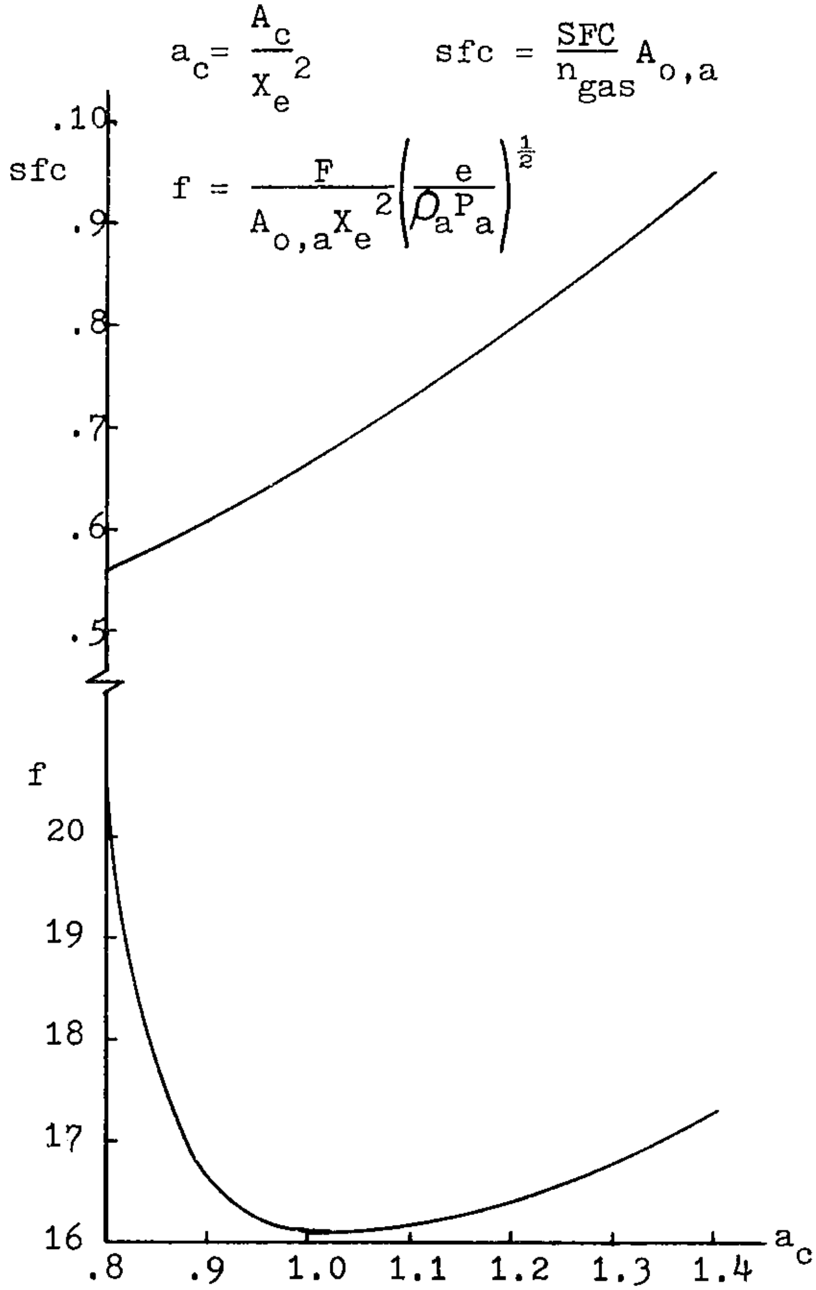

FIGURE 16

a_c vs. bpr, pfc

$$a_c = \frac{A_c}{X_e^2} \quad bpr = \frac{M_{o,p}}{M_{o,c}} \quad pfc = \frac{F_c}{F}$$

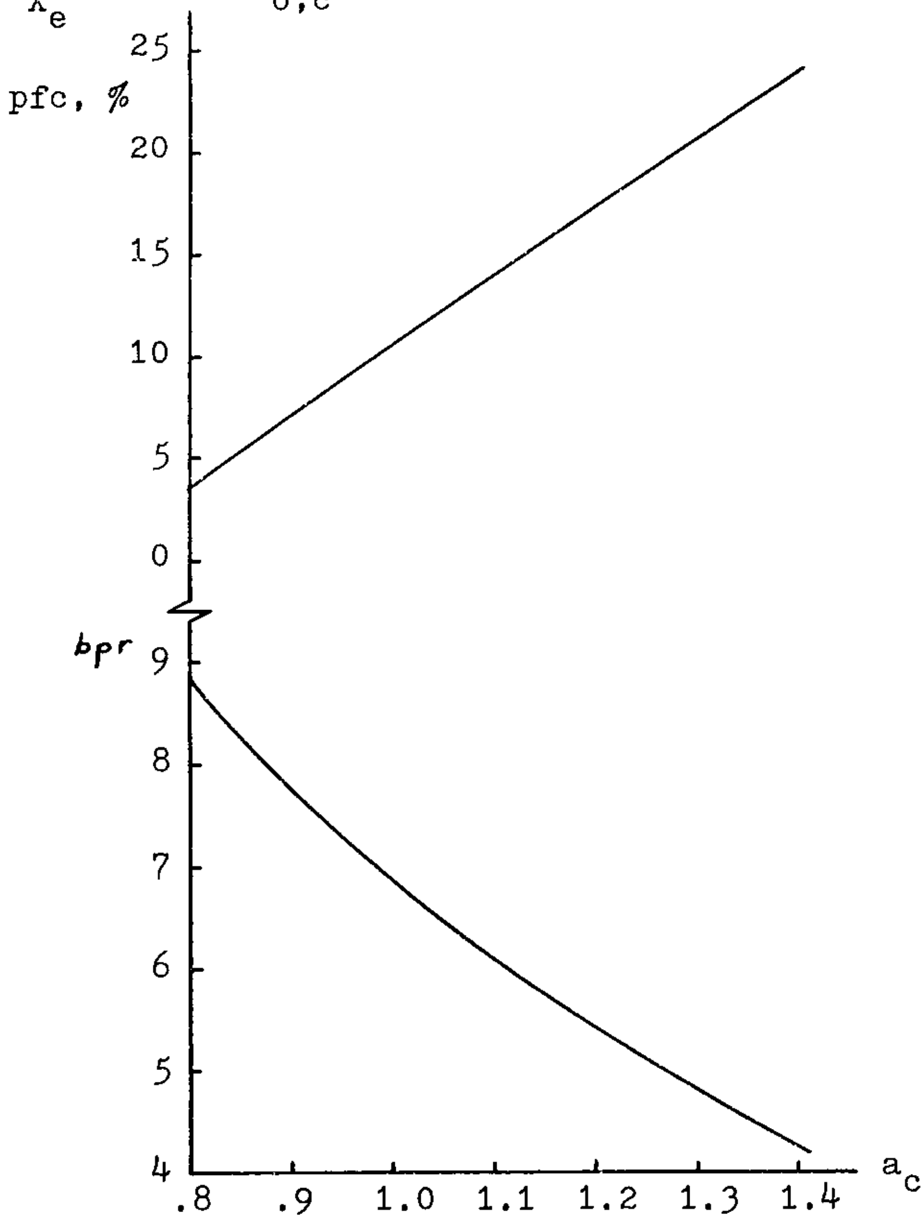

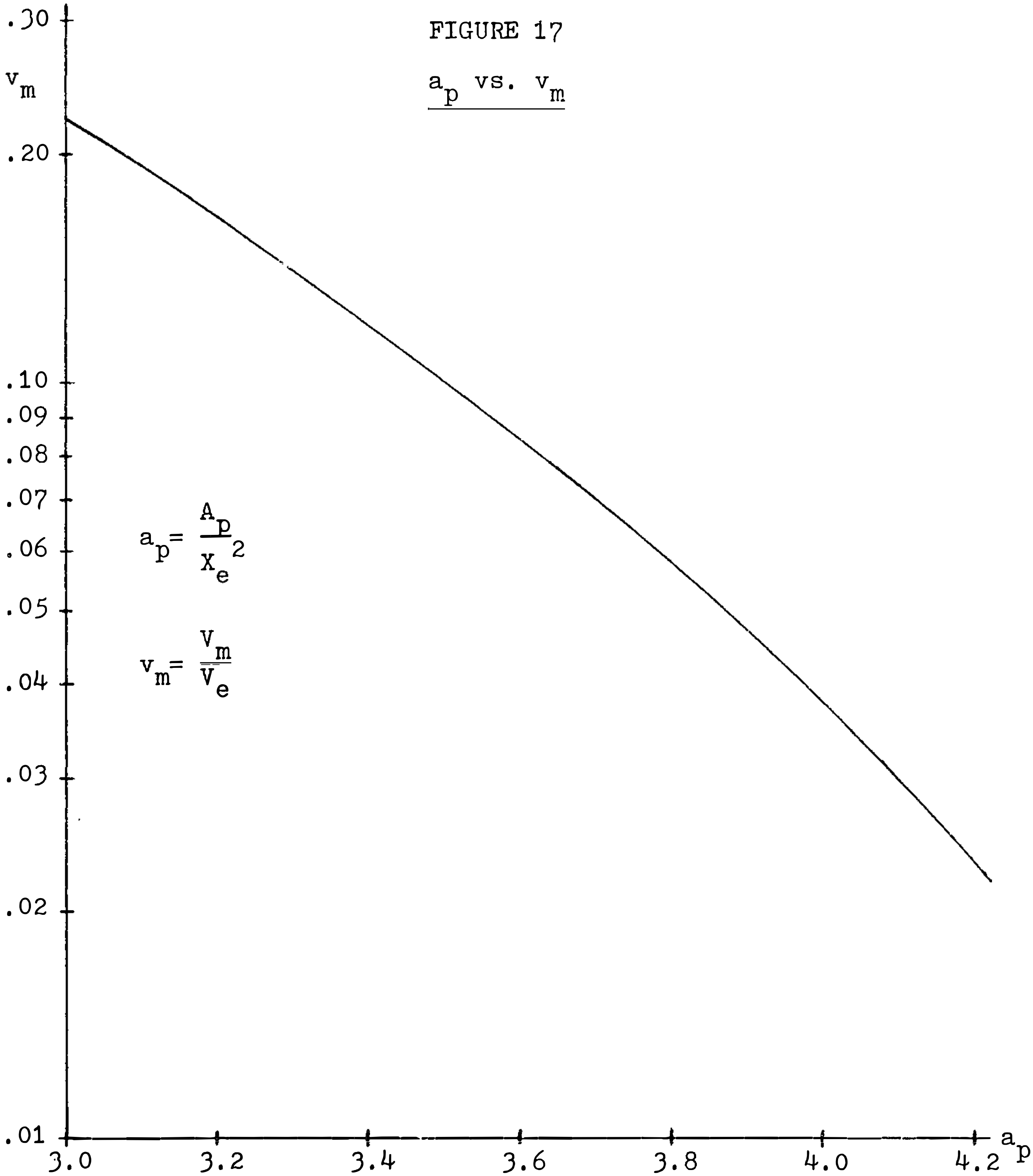

FIGURE 17
a_p vs. v_m
.30
v_m
.20
.10
.09
.08
.07
.06
.05
.04
.03
.02
.01
a_p = A_p / X_e^2
v_m = V_m / V_e
3.0
3.2
3.4
3.6
3.8
4.0
4.2
a_p

FIGURE 18

a_p vs. f, sfc

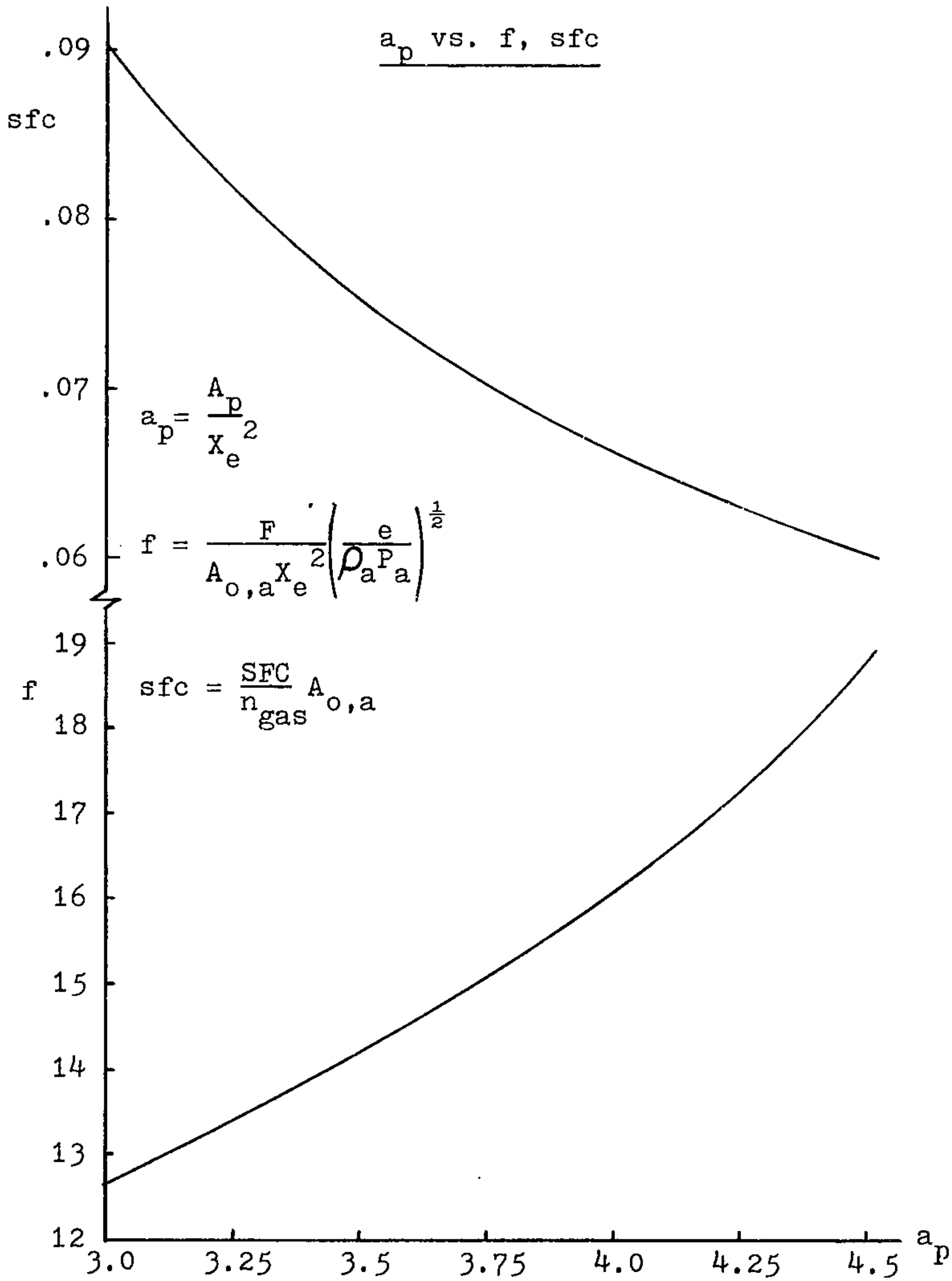

FIGURE 19

a_p vs. bpr, pfc

$$a_p = \frac{A_p}{X_e^2} \qquad bpr = \frac{M_{o,p}}{M_{o,c}} \qquad pfc = \frac{F_c}{F}$$

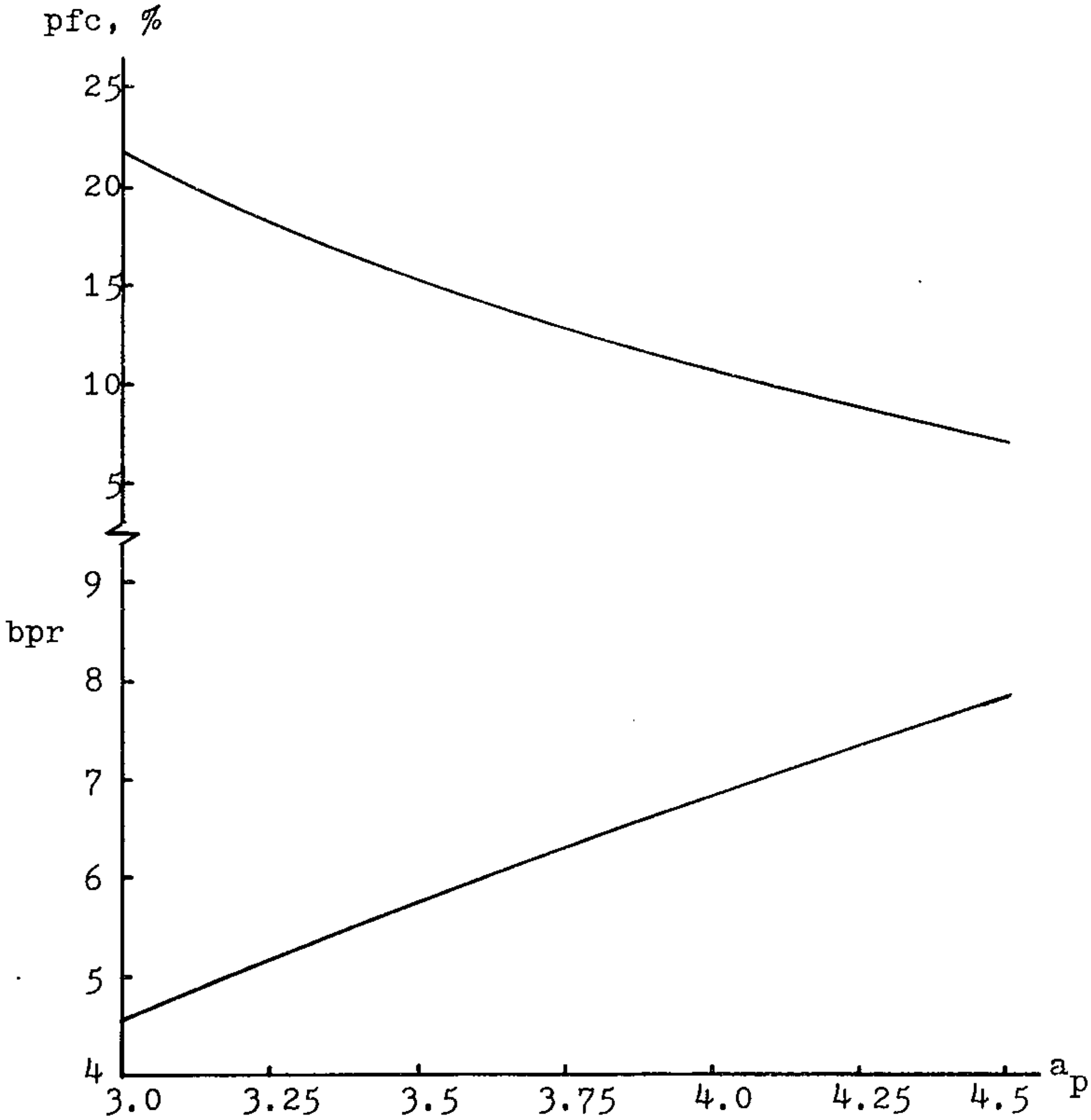

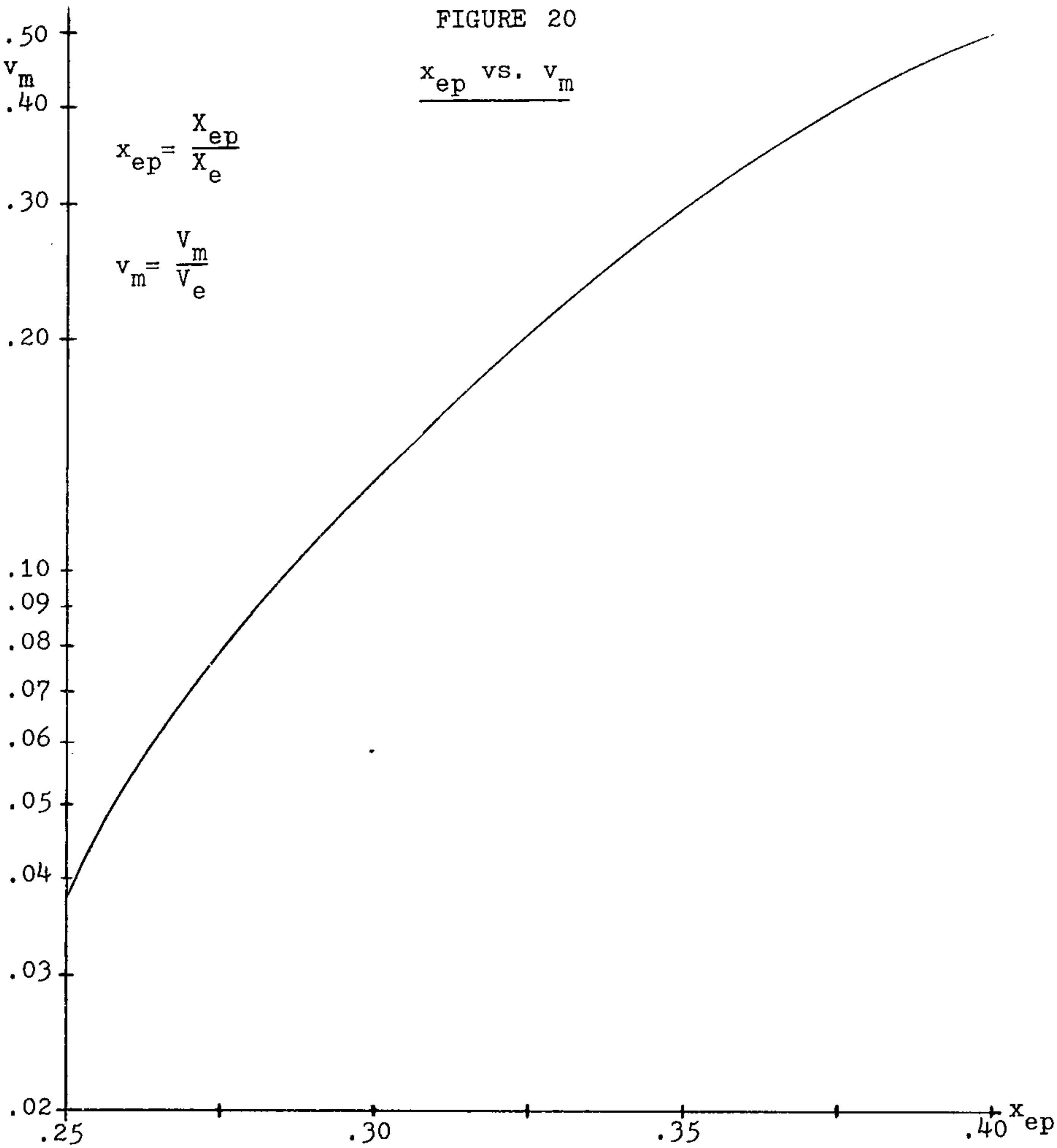
FIGURE 20
x_{ep} vs. v_m
v_m
$x_{ep} = \frac{X_{ep}}{X_e}$
$v_m = \frac{V_m}{V_e}$
.50
.40
.30
.20
.10
.09
.08
.07
.06
.05
.04
.03
.02
.25
.30
.35
.40
x_{ep}

FIGURE 21

x_{ep} vs. f, sfc

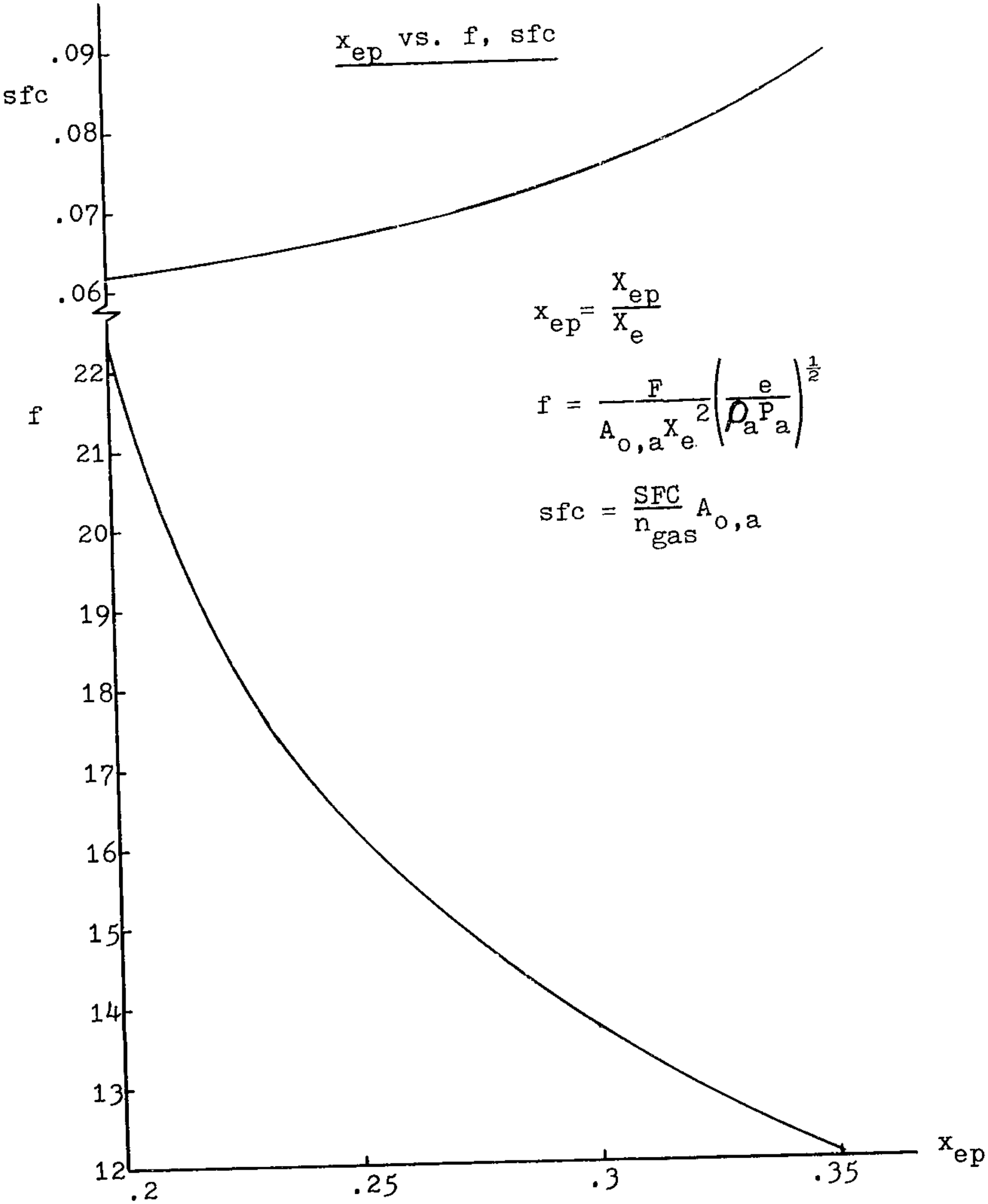

FIGURE 22

x_{ep} vs. bpr, pfc

$$x_{ep} = \frac{X_{ep}}{X_e} \qquad bpr = \frac{M_{o,p}}{M_{o,c}} \qquad pfc = \frac{F_c}{F}$$

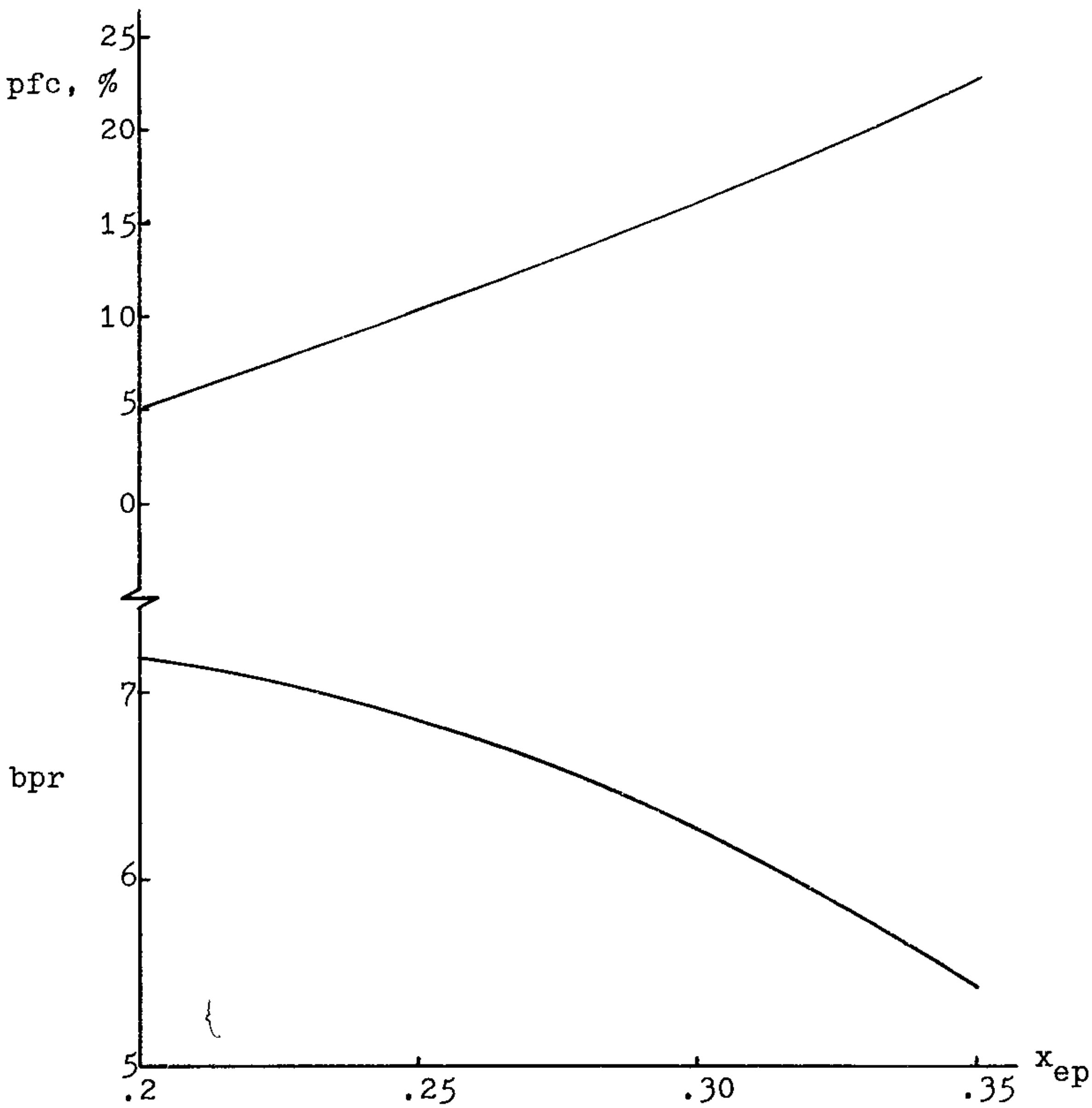

FIGURE 23

x_p vs. v_m

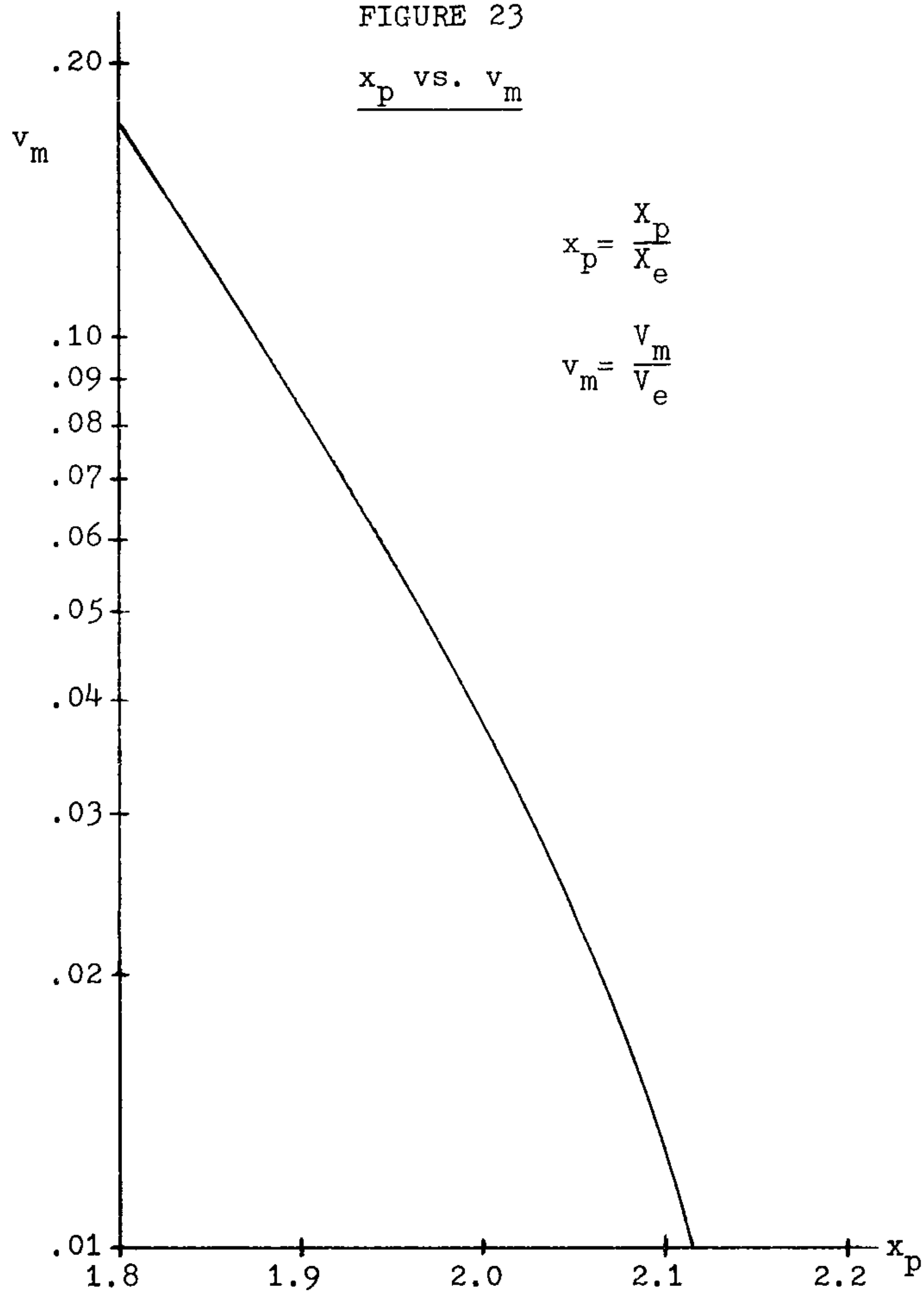

FIGURE 24

x_p vs. f, sfc

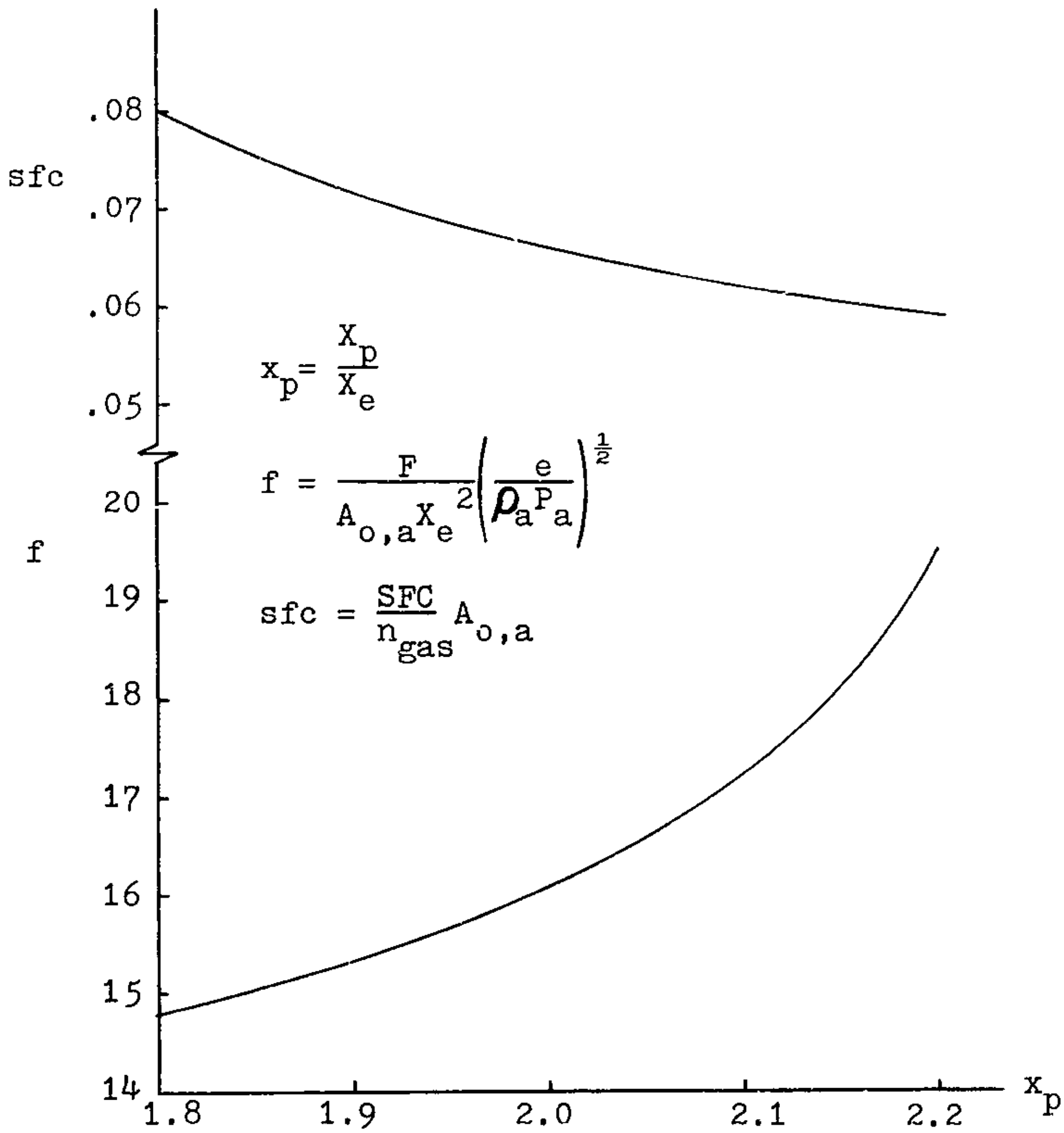

FIGURE 25

x_p vs. bpr, pfc

$$x_p = \frac{X_p}{X_e} \qquad bpr = \frac{M_{o,p}}{M_{o,c}} \qquad pfc = \frac{F_c}{F}$$

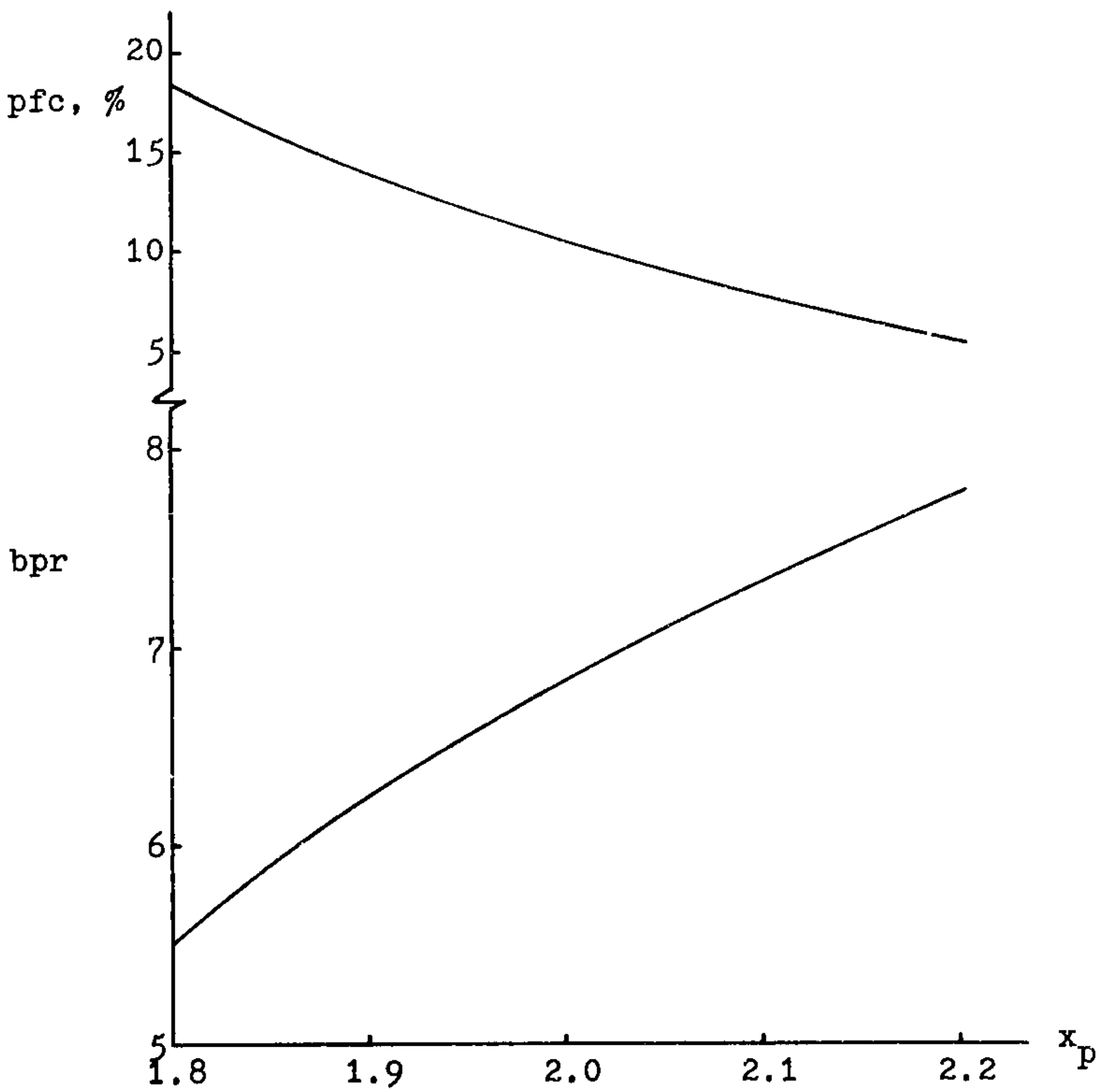

FIGURE 26

bpr vs. f

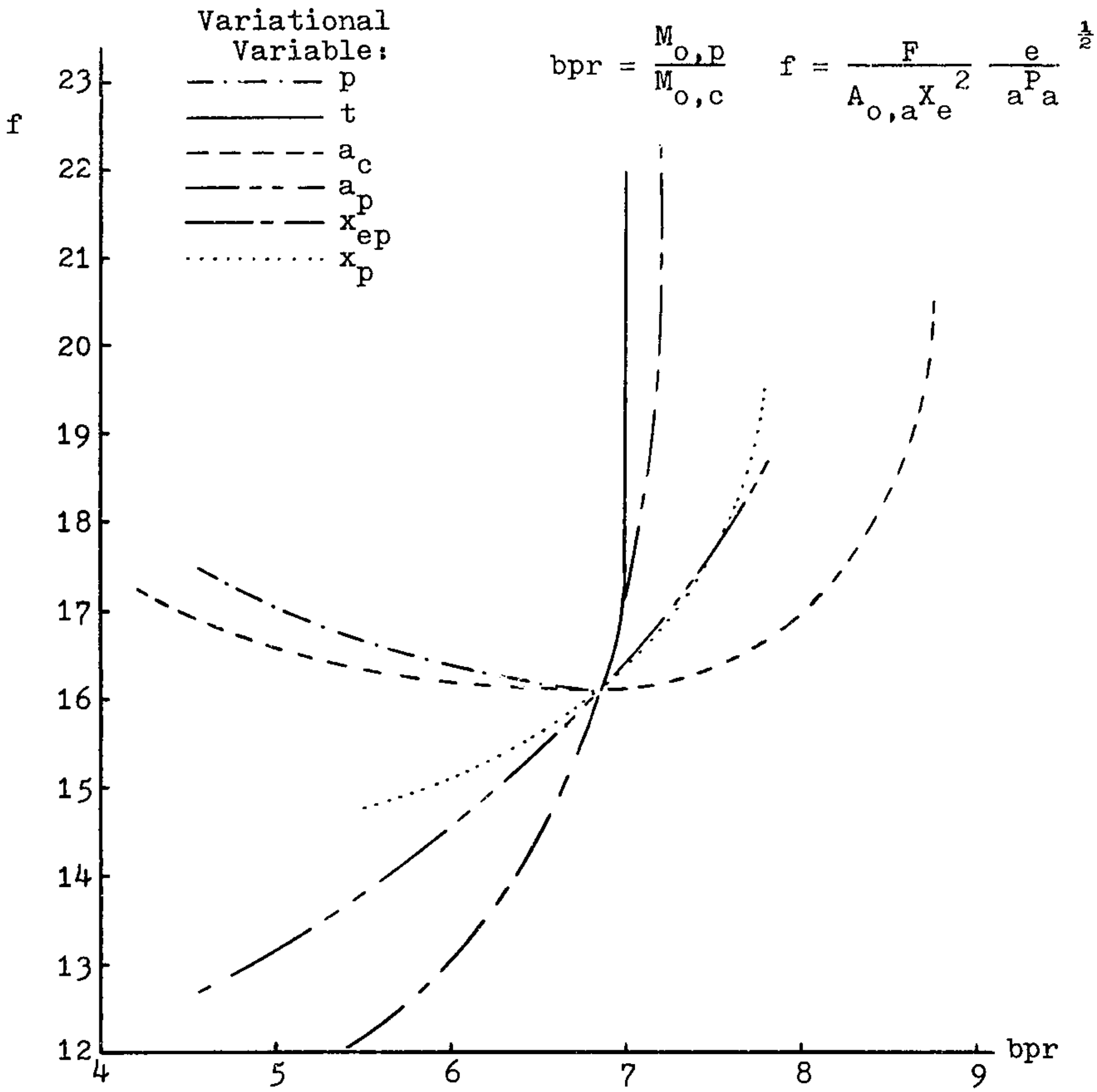

TABLE 1

PROTOTYPE ENGINE CHARACTERISTICS

Combustion diameter, D_c	.281 ft
Density ratio, ρ_{pt}/ρ_a	1000
Combustion exhaust length, X_e	.203 ft
Pump exhaust length, X_{ep}	.033 ft
Effective pump chamber length, X_p	.213 ft
Pump diameter, D_p	.724 ft
Piston mass, M_{pt}	6.71 lbs
Engine speed	7955 cpm
Exhaust Mach number	
Pump	1.815
Combustion chamber	1.810
Bypass ratio, bpr	5.79
Percent thrust by combustor, pfc	14.7%
Weight of engine ($4M_{pt}$)	26.8 lbs
Thrust, F	109 lbs
Specific fuel consumption, SFC	.465 lb/hr-lb
Thrust/Weight	4.06
Fuel flow	50.7 lb/hr
	=8.4 gal/hr